MSc Thesis

Analysis and Evaluation of Three-dimensional Geology Mechanical Model Experiment

Author: Yuantong Zhang

Supervisor: Professor Renshu Yang

Date(06/06/2018)

School of Mechanics and Civil Engineering
China University of Mining and Technology (Beijing)
Beijing Haidian district Xueyuan Rd, Ding 11.
Lijian Building 401
Phone: +86 18810544955

Declaration of Authorship

„I declare in lieu of oath that this thesis is entirely my own work except where otherwise indicated. The presence of quoted or paraphrased material has been clearly signaled and all sources have been referred. The thesis has not been submitted for a degree at any other institution and has not been published yet."

Abstract

Three-dimensional geo-mechanics model test is one of the effective means to solve the problems of underground geotechnical engineering，it can be intuitively, qualitatively and quantitatively reflect the force and structural characteristics of crude rock mass, the relationship between rock mass and underground engineering structure.MEC-3D model test system ,which developed by China University of Mining (Beijing), is capable of static experiment such as tunnel excavation and dynamic experiments, but because of the limit of model materials, there are few research in the dynamic part. This paper aims to research a kind of materials which has such properties as high density, high strength and fast solidification to facilitate the dynamic experiments.Based on this situation, the paper focus on research of similar materials of model experiment. First, introduction of similar criteria and MEC-3D model test system ,which developed by China University of Mining (Beijing), this paper puts importance on its loading system and characteristics. Second, make orthogonal experiment plan to measure physical mechanical parameters in order to analysis property of similar materials. According to certain references, finally use quartz sand, gypsum, cement and iron concentrate to constitute new materials, and water content is another important parameter. make enough mount of standard samples, using universal testing machine to get sample's statics parameters, use Hopkinson Bars Technique to get sample's dynamic parameters, such as density, cohesive force, uniaxial compressive strength, elastic modulus, speed of longitudinal wave, dynamic strength, then use range method and variance method to analysis every parameter's sensitivity and integrity. Finally in order to solve safety problem during dynamic model experiment, numerical analysis is used to evaluate the reaction wall of test machine, determine maximum deformation and stress concentrated area under the worst situation, support a safety reference to the experiments in the future.

Software Abqus 6.14 is used to build the numerical model, simulate the situation where static load and dynamic load happened together.

Key words: Similar material, Model experiment, Strength check, Numerical modeling

Content

Chapter 1: Introduction

1.1 Research background and research significance

There are many methods used to study underground geotechnical engineering, such as theoretical research, field experimental research, numerical simulation theoretical calculation, and similar simulation experimental research. The theoretical research is based on mechanical research, proposes appropriate assumptions, simplifies the original original rock conditions, and does not have significant guiding significance for the field, and is for deep mining projects. Because the rock mass involved in it is in the harsh Geological environment of the "three-high disturbance", resulting in the formation of complex structures and structural characteristics within the rock mass, it has not been possible to accurately describe its constitutive relationship using appropriate theories.[1] At the same time, due to the large degree of disturbance to the strata and the interaction between the engineering structure and the surrounding rock medium, the theoretical research on deep mines is more complicated. On-site test studies can directly conduct relevant tests at the site, without sampling, and avoid disturbance and impact on the test subjects by a series of measures such as drilling sampling, but it is relatively difficult to effectively control the boundary conditions during the test process, such as testing the drainage conditions of the surrounding soil layers. The field actual test cycle is long and time-consuming, the work task is heavy and the input capital is more and more costly. At the same time, the field test conditions are strictly required. Therefore, the field test is very limited. [2-5] In terms of test results, the field measurement is limited by the measurement distance, which makes it difficult for the test results to characterize the changes in the internal characteristics of the rock mass and can't extend the non-measurement area. These are all problems that need to be solved by the field measurement. The rapid development and effective combination of numerical simulation theory and computer hardware provide a powerful tool for the mechanical analysis of deep rock mass, but it is constrained by the rock mass constitutive relationship, some key parameters, software analysis theory, and computer hardware facilities. It is necessary to simplify the complex numerical model of deep rock mass. The three-dimensional geomechanical

model test can qualitatively and quantitatively analyze the interaction between the engineering mechanism and the deep rock mass, provide the necessary theoretical and key parameters for numerical analysis, and verify the results obtained by numerical simulation.[6-7]

Therefore, geomechanical model tests can be used to explore many problems that are difficult to explain by theoretical methods at present, and provide a basis for the establishment of new mathematical models and constitutive relations. The study of three-dimensional geomechanical model test is one of the effective research methods for studying underground geotechnical engineering problems. It can intuitively, qualitatively, and quantitatively reflect the mechanical characteristics and structural characteristics of rocks or rock masses, as well as the relationship between rock masses and underground engineering structures.

In addition, the development of Chinese science and technology has started late, science and technology are not perfect, and material selection in model tests is to a large extent an important factor that affects the final test results, but most of the model test materials in China are used for the study of statics tests. The research and results on the dynamics of measuring materials such as elastic modulus, uniaxial compressive strength, cohesive force, and longitudinal wave velocity are relatively rare, especially when the model test encounters blasting related problems. In order to make up for this deficiency, this paper designs the dynamic test material suitable for this test machine on the basis of the traditional cement mortar materials and the unique properties of the large three-dimensional mine construction model test equipment developed by the China University of Mines (Beijing). The static and kinetic parameters of the test material are measured and analyzed, and then the strength of the geological model tester is checked under the most adverse load conditions. The most unfavorable load refers to the maximum oil source pressure that the system can provide. 5MPa, It is combined with the dynamic pressure formed by blasting under different blasting conditions.

1.2 Research status at home and research

1.2.1The experimental studies of the geomechanical model material

Geomechanical model tests can better reflect the complex characteristics of deep

mine rock masses, such as joints, key faults, etc., and can qualitatively and quantitatively reflect the interaction between the engineering structure and the surrounding affected rock masses. In addition, the test results can be presented directly by a number of collection methods without establishing a complex constitutive relationship, so as to avoid the constraints in mathematical and mechanical theoretical derivation. Therefore, geomechanical model test has been used as an important means to solve various Geological problems in deep mines and has attracted more and more attention from mine experts and scholars at home and abroad. At the International Conference on Rock Mechanics held in 1967 and the 9th International Dam Conference held in the same year, the concept of geomechanical model testing was first proposed. After the meeting, a team of experts led by Prof. E. Fumagalli conducted a number of geomechanical model experiments at the Bergamo Institute for Structural and Modelling Experiments (ISMES) in Italy. The stability of dam shoulder, chamber surrounding rock and slope rock mass is studied by using small pieces of model material. These experiments carried out by the Institute have obtained many very significant results, such as the sliding failure process of the dam's right bank cushion pier obtained from the geomechanical model test of the Itaipu dam, which is basically the same as the field measured results; The crack displacement value obtained from the geomechanical model test of Dacheng Water Conservancy Shuangqu Dam in Taiwan is basically the same as that obtained by field observations. [9-10]The Institute not only has outstanding performance in the popularization and application of geomechanical model tests, but also has made outstanding contributions to the development of geomechanical model tests technology and model test theory. Countries that have made outstanding contributions to geomechanical model tests include the former Soviet Union, the United Kingdom, the United States, Yugoslavia, and Austria. Among them, the team led by R.E. Heuer and A.J. Hendron of the United States conducted extensive and in-depth model tests on the stability of the surrounding rock in the tunnel chamber under static conditions, and for the first time systematically summarized the establishment of similar conditions for the geomechanics model test. Methods and related test techniques, the influence of complex Geological structure on chamber stability is widely studied. [11]

The concept of geomechanical model test has been an important technique in mine research since it was put forward. Geomechanical model test technique mainly focused on plane stress similarity test in the 1960s. It mainly studied the effects of underground

mining activities on overlying rock formations. In the 1970s and 1980s, there was a qualitative change in the test techniques of geomechanics model, and the plane strain model test system and the three-dimensional model test system appeared in the test system. The results have also been obtained in the theory of model experiments, such as the theory of "masonry beam" and the formation law of "three bands" of overlying rock layers on the mining field. Based on the complexity of physical mechanical morphology of rock bodies after engineering disturbance, many experts and scholars in China successfully applied the similarity model test technique to optimize the quality model test of underground engineering activities, and obtained many fruitful research results. By means of geomechanical model test, Suihuiquan studied the effects of underground engineering on the stress and displacement of surrounding rock mass. Dixinxian studied the movement characteristics of the roof rock layer during coal mining in the upper layer of the coal seam, and obtained the development law of the "masonry beam" structure to the top position. Wu Yongping adopted the non-equilibrium fracture statistical method to analyze the unsteady movement and evolution of the rock around the mining face under asymmetric loading. Using the geomechanics model test method, Baiyiru studied the impact of underground mining on surface subsidence. Dengkazhong studied the interface effect between rock formations when the rock mass moved after underground mining. Huyaoqing studied the coal seam mining. The variation of roof stress and displacement [12-16].

After entering the 1990s, the rapid development of computer hardware equipment and the improvement of numerical calculation theory have led to the neglect of geomechanics experimental methods. Because the numerical simulation software can save a lot of manpower, material resources and time, and it is different from the geomechanics model test to change one parameter, the numerical simulation is more convenient to consider the change of parameters. Therefore, many research institutes at home and abroad have abandoned the study of geological model tests and instead conducted numerical simulations. Only a few scientific research units in China still adhere to the study of geomechanical model tests.[17]Although the rapid development of numerical calculation has caused great impact on the geomechanical model tests, the geomechanical model tests are still the most effective means to study the geological conditions and the complex geotechnical engineering of the project itself. Especially in recent years, the test method and the performance of the pressure supply device have been

continuously improved, and the geomechanical model test has accelerated its development. Canadian R.W.I. Brachman, I.D. Moore and other experts used the newly developed geomechanical model test system to simulate buried small-diameter pipelines and studied their structural problems. MaroloC. Alfaro and Ron C.K. Wong studied the fracturing of low permeability soils on the geomechanical model test bench. [18] And In China, a number of scientific research units have conducted in-depth research on geomechanical model tests. Experts who have studied geomechanical model tests include Xiaohongtian, Renweizhong, Zeng Yawu, and Chiyong. Its research content is the stability of the dam foundation and underground factory building of the dam dam in terms of water Conservancy, the support effect of the roadway in the mine, the distribution law of the rock stress in the underground chamber, and the rock mass destruction mechanism [19-24] In the study of some special rock mechanics phenomena, such as rheology and rock explosion, it can only be solved by the study of geomechanical model tests. In this respect, Chenanmin and others used anchor cable to strengthen soft rock for the study of geomechanical model experiments, obtained the creep equation of similar materials, and the relationship between the length of anchor cable tension tonnage with time was studied. Zhangyujun et al. used constitutive theory to establish a mechanical model of the rheological characteristics of Anchorage rock mass in the geomechanical model test. Zhouxiaomin et al. studied the application of artificial frozen strata in engineering practice through geomechanical model tests. Zhujian and Xudongjun studied the rock burst characteristics in underground caverns under different stress paths and the rock failure forms under different stress combinations. In summary, geomechanical model tests and their techniques have been widely used and developed in the field of geotechnical engineering at home and abroad. They are usually used to solve complex geotechnical problems that are difficult to solve by numerical simulation and theoretical research. [25-29].

1.2.2 Research status of model materials

What foreign countries have made outstanding contributions to the study of model materials is the Bergamo structural model test Institute in Italy. Its research model materials are mainly divided into two categories. [30]. First, lead oxide is used as the aggregate material, gypsum is the cemented material, sand and small round stone as the

auxiliary material. The second material uses heavy crystal powder, limestone powder or lead oxide as the main material, epoxy resin as the cementing material, glycerin and water as diluents and humidifiers, diatomite and bentonite as additives. In the late 1970s, when the Institute conducted a geomechanical model test for the Itaipu Dam in Brazil, a new model material was developed. The mechanical properties of the model material strength and deformation modulus were very low[31-33] And ... This model material uses the surface tension of paraffin oil to bind a powdered mixture with a minimum compression deformation modulus of about 60 MPa and a compressive strength of 0.06 to 0.1 MPa.

In China, the Department of Water Resources Engineering of Tsinghua University has studied geomechanical model materials using gypsum as a cementing material, adding starch slurry to partially matched materials to adjust its consolidation strength, and has also tried to use copper powder as an aggravating material. Some experimental studies [34-35]. In addition, Professor Lizhongkui of Tsinghua University also developed NIOS model materials. The main materials of this material are magnetite concentrate powder, river sand, gypsum and cement as binders, water as mixing agents, and other additives. To adjust the various physical mechanical properties of the material. The material material of this model is heavy, its physical mechanical properties can be mediated in a relatively large range, and its performance is relatively stable, and the material source is extensive. [36-39] Professor Hanboli of Wuhan University developed the MIB model material, which uses membrane iron powder as aggregate and alcohol Rosin solution as binder. After mixing the thick aggregate and fine aggregate after adding the film, it is added with a binder and placed in a steel mold to become a model block. Physical mechanics tests conducted on this material show that the weight of the MIB material can reach 3.7 g/cm, which can basically meet the requirements of model materials such as Gaorong, low strength and low elastic modulus. [40] There are also some research institutes such as the Institute of Geology of the Chinese Academy of Sciences, Hehai University, Yangtze River Academy of Water Sciences, Chengdu University of Technology, etc., all have in-depth research on model materials.

There are discontinuous structures such as crevices, voids, and joints inside natural rock masses. Therefore, in addition to selecting suitable model materials when making models, it should also be considered how to simulate the geological structure in natural rock masses when using model materials. [41] Due to the limitations of test conditions and means, it is impossible to copy all the geological formations in the prototype into the

model in the geomechanical model test. At the same time, some non-critical geological formations in the prototype do not need to be reflected in the model body. Therefore, in the geomechanical model test, the discontinuous structure that has a significant impact on the engineering structure should be simulated emphatically. [42-43]Although the geological structure was simplified during the model test, the simulated Geological structure is still an extremely complex problem. Many experts at home and abroad have carried out a large number of model tests on the geological structure and obtained some research results. For clay sandwich viscous sliding can be simulated with grease coating, while plastic sliding can be simulated with talc coating[44-45] And ... Although many studies have been made on similar materials at home and abroad, there are still many problems waiting for us to solve in terms of model materials. In particular, the simulation of the Anisotropy of rock masses and the discontinuity of rock masses is still under exploration. [46] The study of geomechanical model materials, including physical mechanical properties test content and test methods, is still in the exploration stage, and many problems need to be further studied

1.2.3 Dynamic experiments in rock mass

In aviation, aerospace, automobiles, transportation, packaging and other military and civilian fields, engineering materials may encounter impact loads such as explosions and high-speed impacts. Understanding the mechanical response of materials under impact and blasting loading conditions will greatly contribute to the engineering application and engineering design of these materials [47].

First of all, we know that the statics theory of solid mechanics studies solid media in a state of static equilibrium, based on the premise that the inertia of the medium microelements is ignored. This is only permissible and correct if the load strength does not change significantly over time. With the short period of its load as the key feature, the motion parameters change significantly on the short time scale of milliseconds, microseconds and even nanoseconds. Under such dynamic load conditions, the microelement coordinates of the medium are in a dynamic process that changes rapidly with time. This is a dynamic problem. It is necessary to consider the inertia of the dielectric microelements, which leads to the study of the wave propagation of the corresponding force. [48-50].

All solid materials have deformability and inertia. When they are subjected to external loads that change over time, their motion process is always a process related to the propagation, reflection, and interaction of stress waves. In the statics problem of deformable solids that ignore the inertia of the medium, it is only allowed to ignore the process of studying the propagation and interaction of stress waves before the static balance is reached, but instead pays attention to studying the results after the stress balance is reached[51-52] In the problem of rigid body mechanics that ignores the deformability of the medium, when the propagation speed of the stress wave tends to be infinitely large, it is not necessary to consider it again. For deformable solid media under explosive impact load conditions, the load has changed significantly or even been used due to the fact that the load has changed significantly on the same or lower time scale compared to the time required for the stress wave to pass through the object's characteristic length. Over, and under this condition, the motion process of deformable solids is often what we care about. Therefore, we must consider the propagation path and propagation process of stress waves[53].Secondly, the characteristics of the strong impact load that has significant load changes on the short time scale must mean high loading rate or high strain rate at the same time. A large number of experimental studies show that the mechanical behaviors reflected by materials at different strain rates are often different. In terms of material deformation mechanism, in addition to the ideal elastic deformation can be regarded as transient response, other types of inelastic deformation and fracture are non-transient responses that are developed and carried out at a limited rate. For example, the movement process of dislocation, the diffusion process caused by stress, the evolution process of damage, the expansion and propagation process of cracks, etc., so the mechanical properties of the material are essentially related to the strain rate of the material. Usually, with the increase of strain rate, the phenomena such as increasing the strength limit, decreasing the extension rate, increasing the yield limit, yield lag, and fracture lag have become more obvious[54] .Therefore, in addition to the inertial action of the dielectric particles mentioned above, another key reason why the mechanical response of the object under the explosion impact load and the mechanical response under the static load are the dynamic mechanical properties and static mechanical properties of the material itself at high strain rates. Different, That is, the correlation between the material constitutive relationship and the strain rate. From the thermodynamic point of view, the stress-strain process under static load is close to the isothermal process, and the

corresponding stress-strain curve can be approximated as an isothermal curve. The dynamic stress-strain process under high strain rate is close to the adiabatic process. Therefore, it is a thermodynamic process with temperature changes. The corresponding stress-strain curve can be approximated as an adiabatic curve. In this way, if the dynamic response of a deformable solid under the explosion impact load is compared with the static response, it actually contains both the inertial effect of the dielectric particle and the strain rate effect of the material constitutive relationship. [55]

In 1914, B. Hopkinson proposed a clever method to study and measure the pressure-time relationship at the end of the bullet or when the explosive exploded. The device used is called Hopkinson pressure bar, sometimes abbreviated as HPB.

Before World War II, there were not many experts studying dynamic compression loading problems, only G.I. Taylor came up with a method to measure the dynamic compression strength of materials in the late 1930s. The Taylor method is based on certain assumptions, mainly assuming that the material is rigid-ideal plasticity. Using the basic concept of one-dimensional wave propagation, a cylinder is used to hit a rigid target, and then its deformation is measured, and finally the material's dynamic compression yield stress is measured.

In 1948, Davies analyzed the stress wave propagation in the Hopkinson rod, made some adjustments, and invented the use of capacitance to measure the stress pulse in the rod.

In 1949, Kolsky first changed the Hopkinson pressure bar into a separation type and used it to study the dynamic mechanical response of the material at high strain rate and its mathematical model, the dynamic constitutive relationship of the material, and successfully developed the separate Hopkinson pressure bar.(SHPB, Sometimes referred to as the Kolsky pole) technology. In the 1950s, people used experiments to verify St. Venant principle, so that the strain pulse in the rod can be measured with a strain sheet attached to the surface of the rod.

1.3 Main content of the research

Geomechanical model tests in China have a lot of statics, and dynamic tests are rare because of the lack of suitable dynamic similar model materials. The three-dimensional geomechanical model test of deep mine in our school has long been used for static tests.

In order to guarantee the safety of dynamic tests, it is necessary to check its strength. In order to solve the problem of the lack of performance of dynamic model materials, based on the default cement mortar materials and relying on the unique properties of the three-dimensional geomechanics model tester, the dynamic test materials used by this tester are designed. The test materials need to meet the capacity. Major, fast condensation, the integrity is good, and the cracking caused by hydration heat is less.

1) Considering the great but different influences generated by the mass ratio of cement and gypsum, quartz sand and gelatinizer, and the quantity of iron ore powder and water content on the basic physical characteristics of model material, orthogonal tests are applied, instead of traditional test method, to analyze the test result by range method and variance method and get the influences of different material, by which all test results can be got through fewer proportioning tests. During the design of the test, the mass ratio of quartz sand and gelatinizer (A), the mass ratio of cement and gypsum (B), the quantity of iron ore powder (C) and water content (D) are set with four grade respectively.

2) Static and kinetic tests are performed on the preserved specimens to obtain relevant mechanical parameters, as well as cohesive forces, uniaxial compressive strength, elastic modulus, longitudinal wave velocity, and dynamic compressive strength. The order of the influence of four factors on the physical mechanical properties of model materials was discussed by using the methods of extremely poor analysis and variance analysis.

3) Modeling using Sketch Up software and introducing it into Abqus 6.14 software for numerical analysis to simulate the most adverse loads (both dynamic loads generated by blasting and the minimum static loads provided by the test engine's oil source system), Limit deformation that a three-dimensional geomechanics model tester can withstand.

1.4 Technical route

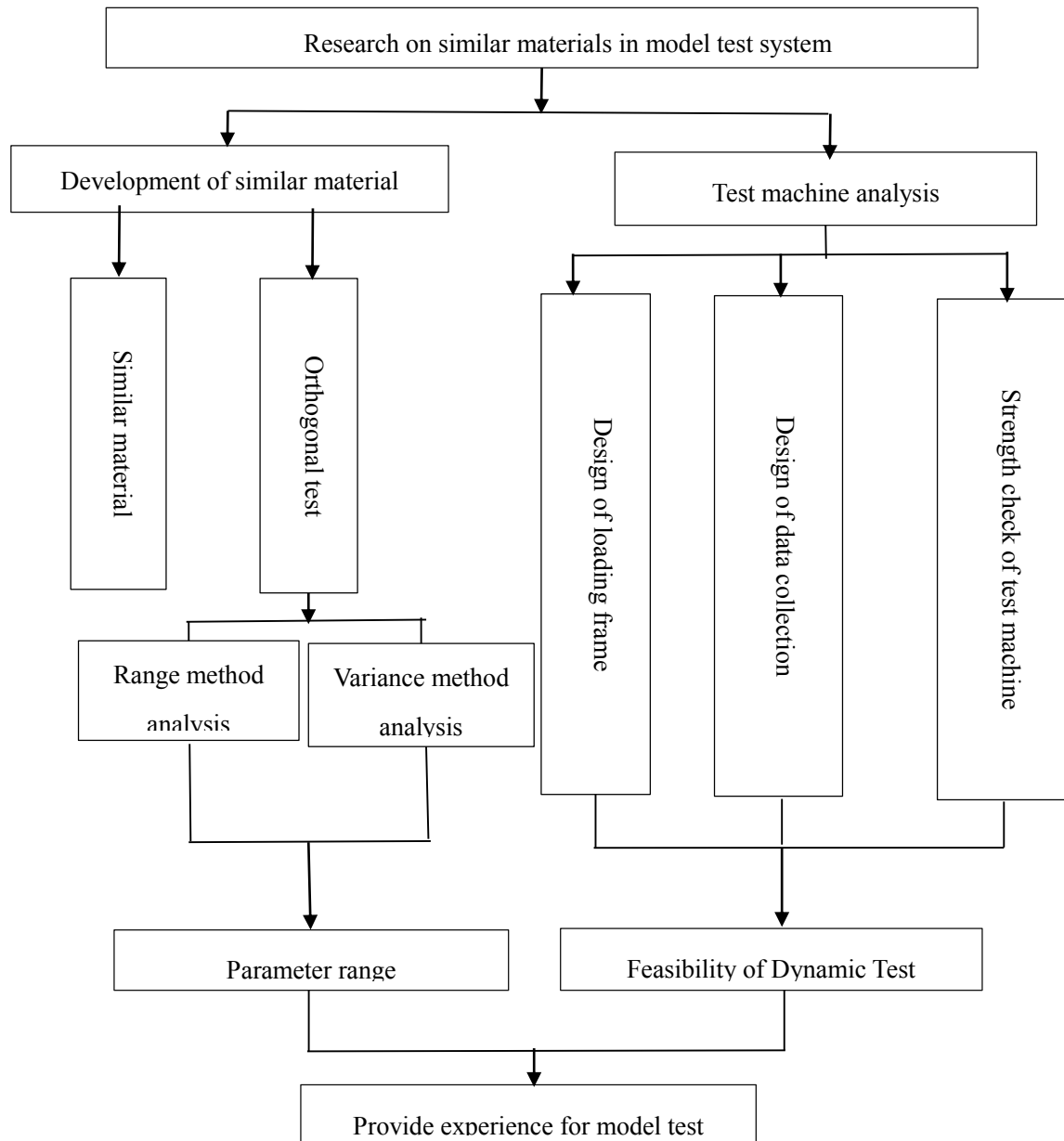The technical route is as follows,

Fig.1.1 The technology roadmap

Chapter 2: Theoretical Basis for Geomechanics Model and Introduction of Laboratory System

2.1 Similarity theory

Experimental research can help people understand the world and make the world become better. However, some tests are too large in size and complex in mechanical properties, it is hard to research through physical tests. So it requires that we seek new test methods to achieve the purpose of the test and apply similar theories to similar simulation tests. It is an important practical way to solve problems. The model test is based on the similarity theory, established the model by reasonable means, and puts it under different test conditions to carry on the research, which has the advantages of low cost, high efficiency and high convenient. After the emergence of similar theories, countless scholars research and practice it, the theory is developed and improved continually, and is applied to scientific research, making outstanding contributions to the development of human scientific and technological civilization.

2.1.1 Concept of Similarity

1) Geometric similarity

The similar concept originally comes from the geometric similarity in mathematics. If two objects are similar in geometric sense, then they mean that their corresponding parts are proportional, and the proportion of each corresponding parts is equal and a constant. This similarity is called geometric similarity. If we use l_1'、 l_2'、 l_3'……; l_1''、 l_2''、 l_3''……to represent the corresponding edge length, then its geometric expression is,

$$\frac{l_1'}{l_1''} = \frac{l_2'}{l_2''} = \frac{l_3'}{l_3''} = \cdots\cdots = C_L \tag{2.1}$$

C_L is a similar constant in the equation.

2) Physical similarity

There are already geometric similarities, then extending similar theories to physical parameters, if the physical quantities on the corresponding parts of the two systems

correspond to each other with certain ratio, then the two systems are physically similar. In this case, if we use U_1'、U_2'、U_3'······；U_1''、U_2''、U_3''······to represent the corresponding physical parameters in the two systems then its physical its physical expression is,

$$\frac{U_1'}{U_1''} = \frac{U_2'}{U_2''} = \frac{U_3'}{U_3''} = \cdots \cdots = C_U$$

(2.2)

C_U is a similar constant in the equation，the subscript U represents any kind of physical parameters。

The physical process will be changed with time and the progress of the project, and status at the beginning of the process or initial state often has important influence on physical process, what's more, the surrounding media and contact conditions will also have a certain impact on the system. Therefor in the two similar systems, their parameters such as time, initial state and boundary conditions must also be similar.

3) Mathematics similarity

The regularity exists in various phenomena in the natural world and it is an important tool for human beings to understand and explore this world. No matter it is same or different physical phenomena, they both have similarity. Even if some physical phenomena are different in nature, they have the same form of mathematical expressions that can reflect their own laws, or they have the same mathematical expressions, but the physical properties they describe are totally different, it is called mathematical similarity.

2.1.2 Three laws of similarity

1) First law of similarity

In similar phenomenon, their single value condition are similar, and their similar criteria have the same proportion coefficient.
This conclusion results from similar having such properties, as followed,

<1> Similar phenomena must be carried out in geometrically similar system, and at all corresponding points in this system, the ratio between the same indicator parameters that express the characteristics of the phenomenon is a constant, which means the similarity constant is equal.

<2> Similar phenomenon obey the same laws in the nature, so the parameters that express phenomenon's properties are bound by some certain nature laws, there must be certain relation between them. If those relation can be presented by mathematical equation, then those equation in similarity phenomenon is same.

The above <1> illustrates meaning of similarity, but it could only explain the similar definitions, it does not find the laws that similar phenomena commonly obey; the above <2> provides a method, which illustrate the similar criteria can be obtained by transformation of similar equations describing phenomena, and it can be concluded that "Similar phenomena have the same value of their criteria"

2) Second law of similarity

If there is an equation that describes a certain phenomenon：

$$f(a_1, a_2, \cdots\cdots, a_k, b_{k+1}, b_{k+2}, \cdots\cdots, b_n) = 0 \tag{2.3}$$

In this equation：a_1，a_2，……，a_k stand for basic parameters；b_{k+1}，b_{k+2}，……，b_n stand for the export parameters that have a certain number of factors，n > k。

The dimensions of all the physical equations are homogeneous, then formula (2.3) could be converted to a non-factorial standard equation：

$$F(\pi_1, \pi_2, \cdots\cdots, \pi_{n-k}) = 0 \tag{2.4}$$

We can get follow conclusions: (i) Normative equation is a function that can express any similar phenomenon; (ii) Number of criterion is (n-k); (iii) criterion is homogeneous.

It is known from the second law of similarity that the criterion equation can be obtained from the transformation of equation that describes the nature phenomenon. Therefore the phenomena that can be presented by mathematical equations can all be expressed in criterion equation and discussed in a deep way. Moreover, second law of similarity can also be used to infer criterion equation, even though the phenomenon only have parameters without mathematical equations. The number of required criteria can also be calculated from the second similar law, and the method of processing and analyzing test's results can also be obtained.

3) Third law of similarity

When the single value conditions of the phenomenon are similar and the similar criteria coefficients composed of single value conditions are the same, we say that this phenomenon is similar. The third law of similarity clearly specifies the sufficient necessary conditions for the similarity of two phenomena. If the two phenomena are similar, it is necessary to meet certain conditions, that is, the corresponding single value conditions are similar, and the similar criteria composed of single value conditions are equal. If the above two conditions are satisfied, the test results obtained by the model test can be applied to other new phenomena without the need for repeated experiments, so as to achieve the purpose of reducing the test cost.

2.2 Application of similarity theory in geomechanical model

2.2.1 Basic concept of geomechanical model

The essence of geomechanical model test is based on the similarity theory, using materials which have similar physical mechanical properties of original materials, and constructing a model body with a certain proportion of the size of the prototype. The stress distribution state of surrounding rock mass or surrounding rock movement state is studied in the model body by simulating various geotechnical engineering phenomena, such as excavation engineering and blasting engineering in the model body. For example, the simulation of roadway support can understand the stress state in the support system, and can observe the influence of different support systems and support parameters on the support effect, and provide theoretical guidance for the optimal design of support; Another example is the simulation of excavation and recovery surface, which can understand the effect of daily recovery on the front support pressure of the working surface by controlling the size of each recovery.

The model tests used to study the nature of a real situation in the prototype and the mechanism of its occurrence belong to the qualitative geomechanical model tests. The same factor will have different impacts in different projects. Qualitative and quantitative research and analysis can be carried out by establishing multiple model experiments. In model tests, it is not necessary to satisfy each similar relationship, but only to satisfy the main similarity constant. Because satisfying all the similarity relationships at the same time is unlikely to be achieved in the actual test at this stage. The quantitative model in the geomechanics model requires that the main physical quantities satisfy their similarity constants and indices as much as possible.

2.2.2 Similar indicators and conditions

The core problem of the model test is the similarity between the built model and the actual prototype. There are many differences between the geomechanical model and the ordinary static model. The key point is that the geomechanical model is to study the elastic and ElastoPlastic processes that the model passes through after starting from the load to the destruction. The normal static structure model is to study the state under a certain load. Therefore, the situation of geomechanical model tests is more complex and requires

models and prototypes. From the beginning to the destruction, the stress States and material properties of the two must be similar.

For geomechanical model experiments，here are the parameters that influence it：geometry size L (m)、stress σ（N/m²）、strain ε、displacement δ（m）、elastic modulus E（N/m²）、poisson ration ν、boundary stress σ̄（N/m²）、body force ρ（N/m³）、bulk density γ（N/m²）、cohesion C（N/m²）、internal friction angle φ、uniaxial compressive strength R$_C$（N/m²）。Related similarity constant could be given as follows：

Geometric similarity constant $$C_L = \frac{L_P}{L_M}$$ (2.4)

Stress similarity constant $$C_\sigma = \frac{\sigma_P}{\sigma_M}$$ (2.5)

Stress similarity constant $$C_\varepsilon = \frac{\varepsilon_P}{\varepsilon_M}$$ (2.6)

Displacement similarity constant $$C_\delta = \frac{\delta_P}{\delta_M}$$ (2.7)

Elastic modulus similarity constant $$C_E = \frac{E_P}{E_M}$$ (2.8)

Poisson ration similarity constant $$C_\upsilon = \frac{\upsilon_P}{\upsilon_M}$$ (2.9)

Boundary stress similarity constant $$C_{\bar\sigma} = \frac{\bar\sigma_P}{\bar\sigma_M}$$ (2.10)

Body force similarity constant $$C_\rho = \frac{\rho_P}{\rho_M}$$ (2.11)

Bulk density similarity constant $$C_\gamma = \frac{\gamma_P}{\gamma_M}$$ (2.12)

Cohesion similarity constant $$C_C = \frac{C_P}{C_M}$$ (2.13)

Internal friction angle similarity constant $$C_\varphi = \frac{\varphi_P}{\varphi_M}$$ (2.14)

UCS similarity constant $$C_{R_C} = \frac{R_{CP}}{R_{CM}}$$ (2.15)

The subscript P represents the prototype and the subscript M represents the model. In addition, in the Elastoplast phase,

Residual strain similarity constant： $$C_{\varepsilon_0} = \frac{\varepsilon_{0P}}{\varepsilon_{0M}}$$ (2.16)

According to similar theory and dimensional analysis method ：

Balance equation similar criterion：

$$\frac{C_\sigma}{C_\rho C_L} = 1$$ (2.17)

Physical equation similar criterion：

$$\frac{C_\sigma}{C_\varepsilon C_E} = 1 \quad \frac{C_\gamma}{C_\rho} = 1 \quad C_\upsilon = 1 \tag{2.18}$$

Geometric equation similar criterion：

$$\frac{C_\delta}{C_\varepsilon C_L} = 1 \tag{2.19}$$

Boundary condition similar creiterion：

$$\frac{C_\sigma}{C_{\bar{\sigma}}} = 1 \tag{2.20}$$

Materials strength similar criterion：

$$\frac{C_\sigma}{C_{R_C}} = \frac{C_C}{C_{R_C}} = C_\varphi = 1 \tag{2.21}$$

The model that satisfied the above similar criteria is called a completely similar criteria model, but for the model materials R_C、φ、γ、E、C as independent physical quantities, it is difficult to achieve all similar criteria after determining the material of the model. On the other hand, the model that can only satisfy the main similarity criterion, called the basic similarity model, and the geomechanical model belongs to the basic similarity model. The deformation characteristic parameters of each component of the geomechanics model must be considered, that is, the deformation modulus and Poisson's ratio need to be similar, and the strain is generally required to be similar.

In addition to meeting the above requirements such as, boundary conditions, material strength, time is another important parameter. The similarity of time can determine the speed of roadway excavation or the recovery speed of the work surface and the stability time in the geomechanical model test. From Newton's second law, the relationship between the time similarity constant C_t and the geometric similarity constant C_L can be obtained,

$$C_t = \sqrt{C_l} \tag{2.22}$$

2.3 Three dimensional geomechanical model test machine

2.3.1 Introduction of test machine

In order to overcome the deficiency of the model test system, this system provides a three-dimensional model test system for the deep mine construction project. This system can not only carry out ordinary geomechanical model tests. At the same time, it can also

be used to simulate and test the complex Geological conditions such as underground blasting engineering, Highland stress, water-rich engineering, high-speed impact, and radioactive material storage engineering.

The system includes hydraulic loading system, counterforce frame device, intelligent control system and data monitoring system. Hydraulic loading system belongs to servo system and consists of servo oil source and servo actuator. The intelligent control system is composed of full digital controller and servo valve. The counterforce frame device is a loading system made of high quality steel plate, groove steel, I-steel and other materials connected by bolts and weld.

The servo oil source can provide different working pressure for each group of servo actuators to meet the need of different loads on the model. It is mainly composed of fuel tanks, oil pump power sets, filtration devices, electro-hydraulic servo valves, high-precision pressure sensors, pressure gauges, safety valves, cooling devices, and pipelines.

The servo actuator consists of a vertical cylinder and a horizontal cylinder. Each cylinder has its own input-back pipeline and oil circuit switch, which can be connected or disconnected as required.

The counter frame is a "mouth" shape structure consisting of parts such as upper and lower beams, columns, and counterforce support beams.

Horizontal cylinder (back) installs on back loading frame, back loading frame is connected with counterforce wall by pull bar assembly, back loading frame and back counterforce wall is an independent system, when it works, it doesn't have addition load on the left and right surface of the machine.
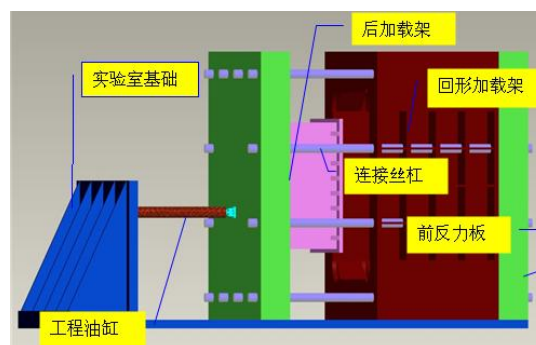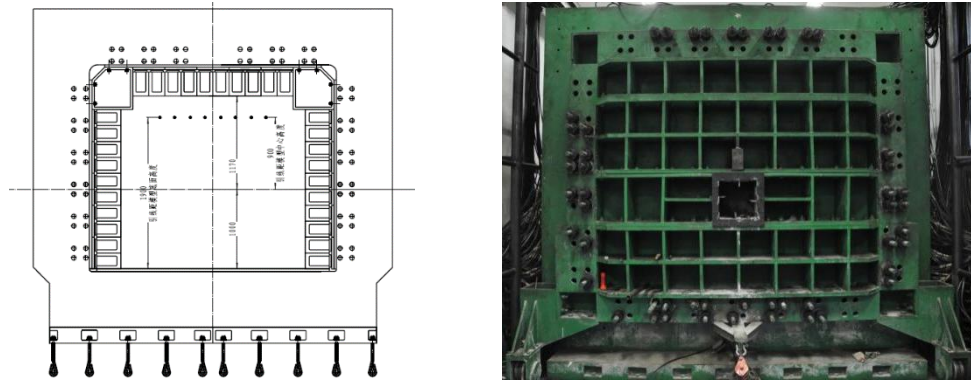
Fig.3.1 The load of framework of test machine

2.3.2 Main technical properties of the test machine

The main technical indicators of the three dimensional geomechanics model test are: 1.The large-scale three dimensional model test and the two-dimensional plane stress model test can be carried out. The maximum size of the model body can reach 2000mm × 2000mm × 1200mm, and the maximum section of the large roadway can be simulated as 400mm × 400mm; 2. The effective pressure that the model can load in the X, Y and Z direction is 5 Mpa, the effective movement of cylinder is 150mm, the load concentration deviation ≤5%, the water head that the test carry out is 0.8 Mpa; 3. In terms of mechanical properties, the loading speed can be continuously adjusted between 0 and 0.15 Mpa, the load constant time ≥168h, and the total power of the test is 40 to 50 kw; 4. The collection system can record the effective pressure, displacement, loading speed, and retention time of the constant load in all direction during model test, the results can be displayed digitally with the operating software in the system.

1. The servo hydraulic oil source system can provide different pressure to the actuator by controlling the flow of the working oil, and achieve the load requirements under different test conditions, as shown in Figure 3.2. The electro-hydraulic servo valve is the D633 electro-hydraulic servo valve of the MOOG Company in the United States. The servo valve is controlled by the EDC220 controller. High-precision pressure sensors can accurately measure the pressure of the oil source in the tubing and display it digitally on the computer through specific processing. When the pressure exceeds the safety pressure of the hydraulic system, the system will automatically unload and reduce the pressure in the fuel tank to avoid excessive pressure on the hydraulic system, mechanical parts or the model body. The temperature detector can pay attention to the temperature of the mailbox at all times, so as to avoid the safety hazards caused by the high temperature of the fuel

tank.
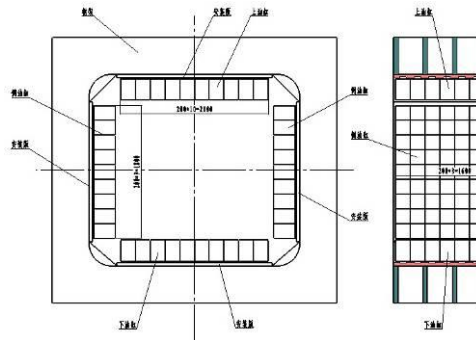
Fig.3.2 Servo actuator sketch map

2. Computer servo control system

The computer's EDC220 full-digital controller can control the entire system in full digital closed-loop and control the target value and speed of the load in real time. The servo controller is the original EDC220 digital controller of the German Doli company. The EDC digital controller is powerful, stable, and has a strong ability to expand.

3. Data acquisition system

In the model test, the strain gauge, pressure box and other electronic measuring instruments are often used to collect data, and the system is equipped with an electrical measuring data acquisition system accordingly. The data acquisition system is made up of nine KD7024 static strain instruments produced by Yangzhou Science and Electronics. Following the pictures 3.3.

Fig.3.3 Data collection system

（4）Displacement measurement device

The deformation of the test object is measured by means of high precision conductive plastic electrode. The deformation of the model is detected by the computer continually.

The deformation of every cylinder and the deformation of every surface can be displayed on the computer screen.

Compared with similar model test systems at home and abroad, the three dimensional geomechanical model test system has the following advantages and innovativeness:

1. The system structure of the test machine is a variable structure. Not only can the two-dimensional plane model test be carried out, but also the three-dimensional model test can be carried out. The same test machine can carry out different dimensions of the test and expand the scope of use.

2. The model tester can simulate the underground blasting test. At present, the blasting similarity model tests are conducted using similar materials without constraints. This kind of environment without containment is very different from the actual underground blasting construction environment, but the loading system has added factors that limit the boundary conditions. It can better reflect the geological disturbance of rock mass and rock formation during blasting.

3. The test machine can simulate the water-rock coupled tunnel (roadway) under water-rich conditions, which provides a platform and tool for the research in this field.

4. The test machine can realize the excavation and support research of simulated roadway (tunnel) under real stress environment. The traditional model test process is to lay out the production model and then carry out the engineering practice such as roadway excavation. Unlike the traditional test process, the model test system can simulate the real stress environment and carry out the original rock stress loading and then carry out the roadway excavation. The simulation of the actual construction of surrounding rock in roadway engineering can reveal its deformation and failure characteristics. In addition, it can realize many excavation methods such as artificial excavation of complex engineering, excavation under blasting conditions, and mechanical continuous simulation excavation.

5. The performance of roadway surrounding rock can be simulated in a wide range of fields. The model tester has a high stress design, which can simulate rock mass with complex joint surface to rock mass with high integrity coefficient, and the surrounding rock and its engineering characteristics under three-dimensional high stress environment.

6. It has good function extensibility. At the beginning of the design, the test machine has a usable interface. After gradually improving its function, it can simulate the thermal rock engineering of deep rock formations under high temperature conditions, and use

freezing method to construct the engineering simulation under high stress and low temperature conditions. The high radioactive waste nuclear waste storage test and the deep rock engineering carbon storage test.

2.4 Conclusion of this chapter

The similarity theory is the theoretical basis of the geomechanics model test. This chapter simply introduces the similarity three theorems from the aspects of similarity theory geometric similarity, physical similarity, and mathematical similarity, and points out the limitations of similarity theory in practical experiments. Then the application of the theory of force similarity in the model test of geomechanics is briefly described, and the three-dimensional model test system for the construction of deep mines developed by the China University of Mining (Beijing) is introduced in all directions.

Chapter 3: Making and parameter analyzing of similar materials

3.1 The choice of similar materials

Even though the physics characteristics of similar materials can be calculated with the help of similarity theory, it is hard to find a material matching all similarity ratios. Therefore the priority of the paper is to find out the factors affecting experiment results.

Bulk material and granular material are available for choice. In the condition of true triaxial test, the similar materials are required to present its statics features and blast effect. The bulk material can coagulate into integrity for one time and not easy to change in volume under high stress, so it's helpful for us to evaluate the blast effect through analyzing the lump size and casting distance. While the granular material need to be compacted for several times. Under shear stress, the relevant dislocation of granule will result in volume changes, which makes it difficult to evaluate blast effect. Besides, considering the experiment period and cost, the similar material shall be easy to be processed, molded and dried, can be bought at a low price and can be recycled as well.

Since the model test is not specialized to any project, the physical characteristics of grade Ⅲ engineering rock mass are taken as standard to prepare modeling materials. According to Tab 3.4, we know that the modeling material's saturated unit weight is 24.5~26.5 kN/m3, cohesive force is 43~94 kPa, modulus of deformation is 375~1250 MPa, uniaxial compressive strength is 1.875~3.75 MPa, tensile strength is 200~282 kPa, Poisson's ratio is 0.25~0.3, and longitudinal wave velocity is 3~4.5 km/s. It is a modeling material with high strength and density.

Based on the pros and cons of modeling materials, cement mortar is applied to serve as main material in this modeling test. According to the researched of domestic and abroad experts and scholars, the similar material made of cement mortar is suitable for blast test of rock and roadways. The small-scale cement mortar modeling test on magnetite conducted by Chinese expert Yang Zuguang and Swedish scholar Agne Rustan shows that the blast to heterogeneous mortar model having a certain intensity could be used to simulate the blast site randomly distributed with small and weak pieces. After that, a Swedish research group, Gert Bjarnholt, made modeling test with nearly one ton cement test block and found that the characteristics of cement mortar itself contributed to the

same blast effect of cement mortar just as the medium-strength rock did. Therefore, it is feasible to choose cement mortar to prepare models in cut blasting model test and the suitable model material can be made through orthogonal tests.

3.2 Orthogonal Tests Scheme

The model material takes quartz sand as main material, cement and gypsum as inorganic gelatinizer, and iron ore powder as density regulator, among which quartz sand is 50-70 mesh; iron ore powder, 400 mesh, manufactured in the iron ore plant in Lingshou County, Hebei province and the density thereof is 44.1kN/m3; Portland cement marked with 42.5; gypsum powder is 3.0 high-strength commonly used for architecture.

3.2.1 Ratio of compounding

Considering the great but different influences generated by the mass ratio of cement and gypsum, quartz sand and gelatinizer, and the quantity of iron ore powder and water content on the basic physical characteristics of model material, orthogonal tests are applied, instead of traditional test method, to analyze the test result by range method and variance method and get the influences of different material, by which all test results can be got through fewer proportioning tests. During the design of the test, the mass ratio of quartz sand and gelatinizer (A), the mass ratio of cement and gypsum (B), the quantity of iron ore powder (C) and water content (D) are set with four grade respectively as following Tab 3.1:

Tab.3.1 Physical mechanical parameters of the grade Ⅲ engineering rock mass

Grades	mass ratio of quartz sand and gelatinizer	mass ratio of cement and gypsum gypsum：cement	quantity of iron ore powder	Water content
	（A）	（B）	（C）	（D）
1	1:1	8:2	5%	15%
2	2:1	7:3	10%	25%
3	3:1	6:4	15%	35%
4	4:1	5:5	20%	45%

Note 1) mass ratio of quartz sand and gelatinizer

Note 2) the influence of the ratio between gypsum and cement on the characteristics of model material

Note 3) water content：percentage of water in total mass of compounding

The mechanical characteristics of material is very important. In order to figure out the proportion of model materials, a suit of specially-made mold is applied in research, including a cylindrical iron double-faced mold ϕ= 50 mm × 100 mm and specimen with internal surface processed leaving slope variance less than 0.05mm. After assembly, all specimen occluded closely to prevent any possibility of collapse or vadose. The volume of specimen is V= $1.9625 \times 10\text{-}4\ \text{m}^3$；total mass thereof is 25 kN/m^3，and the density is ρ=2.55×10^3 kg/m3, accordingly, the total mass of similar material can be determined as m=ρV=$2.55 \times 10^3 \times 1.9625 \times 10\text{-}4$=0.5 kg. The iron ore powder, as an important element in the similar material test, its proportion and mass are showed in the Tab 3.3. The content of the four elements are figured out as Tab 3.3 based on the proportion parameter from orthogonal tests.

Tab.3.2 Percentage and mass of iron ore powder

Percentage	Mass of iron ore powder	Mass of remaining material
5%	0.025 kg	0.475 kg
15%	0.075 kg	0.425 kg
25%	0.125 kg	0.375 kg
35%	0.175 kg	0.325 kg

Tab.3.3 Main parameters' quality in range method experiment

| Proportion No.	Mass of iron ore powder	Mass of quartz sans	Mass of cement and gypsum	
1	75 g	212.5 g	gypsum	170 g
			cement	42.5 g
2	75 g	212.5 g	gypsum	148.75 g
			cement	63.75 g
3	75 g	212.5 g	gypsum	127.5 g
			cement	85 g
4	75 g	212.5 g	gypsum	106.25 g
			cement	106.25 g
5	75 g	283 g	gypsum	113.6 g
			cement	28.4 g
6	75 g	318.75 g	gypsum	85 g
			cement	21.25 g
7	75 g	340 g	gypsum	68 g
			cement	17 g
8	75 g	283 g	gypsum	71 g
			cement	71 g
9	75 g	318.75 g	gypsum	53.125 g
			cement	53.125 g
10	75 g	340 g	gypsum	42.5 g
			cement	42.5 g
11	25 g	212.5 g	gypsum	183.75 g
			cement	78.75 g
12	25 g	283 g	gypsum	96 g
			cement	96 g
13	125 g	212.5 g	gypsum	113.75 g
			cement	48.75 g
14	125 g	283 g	gypsum	46 g
			cement	46 g
15	175 g	212.5 g	gypsum	78.75 g
			cement	33.75 g
16	175 g	283 g	gypsum	21 g
			cement	21 g

The making processes of specimen are as follow:

1. Calculate the amount of quartz sand, iron ore powder, gypsum, and lime in the test according to the ratio determined in advance. Consider the moisture content in the quartz sand if necessary.

2. Weight the amount of each component with an electronic balance as standby.

3. Prepare the test mold and apply silicone oil evenly to the internal surface of the mold for the convenience of demould.

4. Pour the four components into hopper sequentially, and add quantitative water slowly while stirring for 2-3 minutes continuously.

5. Fill the mixed material in the test mold in one time, during which using a spatula to slightly vibrate along the inner wall of the mold and keep the material slightly higher than the mold.

6. Press the glass plate onto the test mold, remove the surplus compounding and air bubbles in it, and smooth with a spatula.

7. After leaving the mold rest for 30 minutes, demould and clean the mold.

8. After the specimen is made, conserve it in room for 28 days.

The making processes of specimen as is shown in the following graphs 3.1.
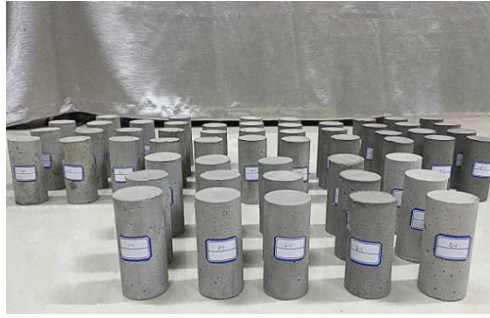

（a）cylindrical iron doubl faced mold
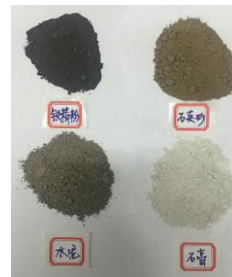
（a）different components of material

（c）stir evenly

（d）keep rest after vibrating

（e）cylindrical specimen

Fig.3.1 Preparation of orthogonal test specimen

3.2.2　The orthogonal test result

"Four factors and four grades" orthogonal table L_{16}（4^4）is applied to determine the test scheme. Namely four factors being arranged with four grades respectively, then there will be 16 matching groups so that every factor at different levels could be evaluated in a balanced and focused way, making the scheme more typical and scientific.

Tab.3.4 Physical mechanical parameters of the grade Ⅲ engineering rock mass

	Factors				Evaluation index			
NO.	mass ratio of quartz sand and gelatinizer（A）	mass ratio of cement and gypsum （B）	Mass of iron ore powder （C）	Water content （D）	cohesive force/kPa	Uniaxial compressive strength/Mpa	Elasticity modulus/Mpa	Longitudinal wave velocity/m/s
1	A1	B1	C1	D4	108.2	3.12	1704	4213
2	A1	B2	C2	D3	105.1	3.52	1577	4552
3	A1	B3	C3	D2	93.4	3.74	1384	4783
4	A1	B4	C4	D1	91.8	4.01	1156	4819
5	A2	B1	C2	D2	80	2.21	903	3817
6	A2	B2	C1	D1	82.8	2.75	965	3439
7	A2	B3	C4	D3	69.8	2.68	843	4147
8	A2	B4	C3	D4	73.3	2.85	885	4102
9	A3	B1	C3	D1	51.5	2.14	682	3692
10	A3	B2	C4	D2	50.1	2.34	634	4038
11	A3	B3	C1	D3	62.4	2.39	775	3258
12	A3	B4	C2	D4	59.8	2.51	724	3854
13	A4	B1	C4	D3	39.1	1.64	375	3471

14	A4	B2	C3	D4	30.1	1.53	298	3304
15	A4	B3	C2	D1	45.5	1.79	489	3150
16	A4	B4	C1	D2	49.5	1.89	586	3065

According to the 16 matching schemes mentioned above on ϕ=50 mm×100 mm standard cylinder specimen, at least 3 specimens shall be made by each matching scheme. Since the volume of specimen is fixed and the density similarity ratio $C\gamma$=1, the density of model material thus can be determined as γ =25 kN/m^3. Therefore, the mass of single cylinder is 2550 kg/m^3 × 1.96×10-4 m^3=500 g and the mass of other materials can be figured out accordingly. The mass ratio of quartz sand and gelatinizer is 1:1; the mass ratio of cement and gypsum is 8:2; the percentage of iron ore powder is 5% and the percentage of water content is 15%. The total mass is 500 g, among which iron ore powder is 25g, leaving quartz sand and gelatinous materials totally 475g. Since the mass ratio of quartz sand and gelatinizer is 1:1, the mass of quartz sand is 237.5g; since the mass ratio of cement and gypsum is 8:2, the mass of gypsum is 190g and cement is 47.5, and the mass of water is 500 g ×15%=75 g. Weight the mass of material respectively with electronic scale and mix them together, then add certain amount of water-dissolved gelatinous materials and fully stir in a cement mortar mixer. After that, add the prepared compounding into the cylindrical iron double-faced molds that have been covered silicone oil evenly on the internal surface respectively, and pound the compounding with poker vibration to release bubbles. The preparation time shall be strictly controlled so that workability and slump of mortar in every specimen can be kept at the same level. Demould after 48-hour natural conservation, then measure the weight and mark with labels. Lastly, measure the basic physical and mechanical parameters after 28-day regular conservation under ordinary temperature, and fill the results in the orthogonal form.

3.3 Measuring and analyzing the physical and mechanical parameters

Curing time: since moisture content has a great influence on physical and mechanical characteristics, it's necessary to weight and record the average of 16 matching schemes every other day and reflect changes with the line graph as is indicated in 3.2. The result indicates that the mass of specimens are decreased with time because of evaporation; after 12 days, most of specimens are dry with little mass variation. The No. 1, 2, 3, 4, 5 and 6

matching scheme have a high content of gypsum and cement, and the active hydration reaction between them consume a large amount of water and the mass of them tend to stable after 10-day conservation. Compared with the other matching scheme, the mass of No. 12, 13, 14, 15, 16 changes slowly with time and become dry after 20-day conservation, the reason for which is that the mass ratio of quartz sand and gelatinizer of them is large while the content of gypsum and cement is small, and the water consumption of hydration reaction is little.
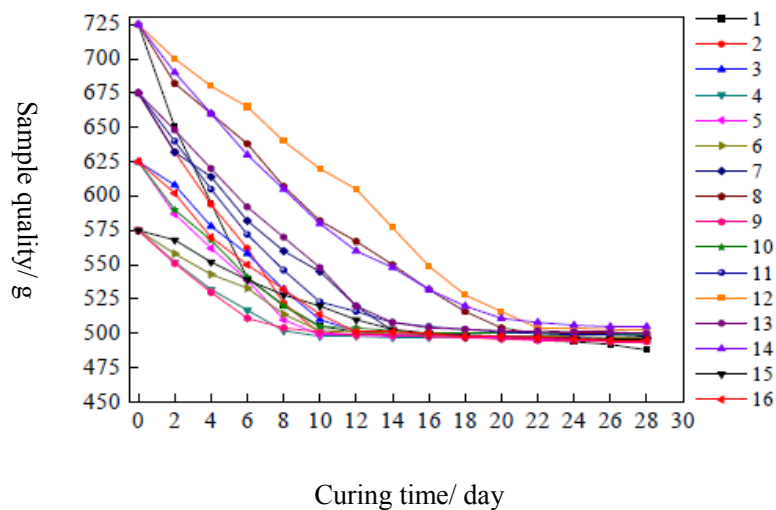

Fig.3.2 Curves of specimen mass and conservation time

Specimen will be ready for ultrasonic test (as is shown in the graph 3.3) after 28-day conservation. The equipment or device involved in this test include Olympus electronic pulse transmitter, DPO 5104B electronic oscillograph developed by Tektronix and 100 KMz nonmetal acoustic transducer for ultrasonic probe. In order to obtain a more accurate longitudinal wave velocity, specimen is firmly fixed between transmitting probe and pick-up probe which are coated with couplant specially used for ultrasonic test. The pulse launched by transmitting probe is received by the pick-up probe after and transferred into electrical signal whose data is collected by micro-computer and reflected by wiggled curve (as is shown in the graph 3.4). With the time period from the launch and receive of ultrasonic wave "t" and the length of specimen "L", the longitudinal wave velocity of model materials could be figured out.
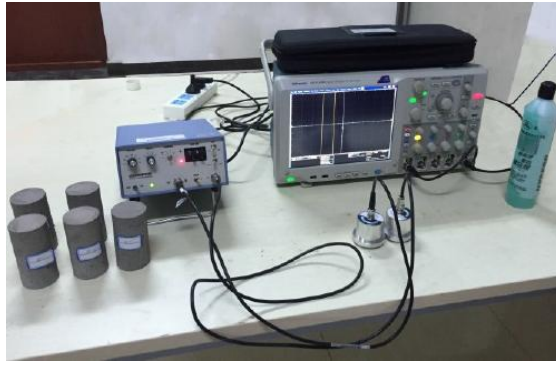
Fig.3.3 ultrasonic test of specimens
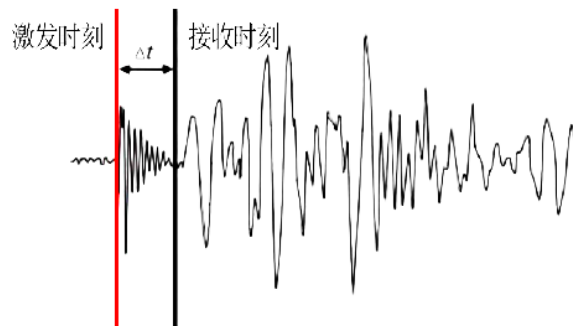

激发时刻 Δt 接收时刻

Fig.3.4 Typical wave of ultrasonic test

MTS-CMT5000 micro-computer is applied to control electronic universal testing machine and measure the uniaxial compressive strength, cohesive force and elasticity modulus of specimens, and fill the average in Tab 3.4. The macroscopic failure characteristics of dried specimen after uniaxial compressive test together with marks of cracks and failure surface reveal that the failure characteristics of specimen and brittle rocks is the same, namely there are typical shear slip surface and tensile fracture surface, besides the tensile fracture surface is nearly parallel with loading direction. With the extension, development and convergence of the tensile fracture surface and shear slip surface, circumferential cracks appear on the surface of some certain specimens and the failure characteristics thereof shows "compression shear failure" and "tensile failure" （as is shown in the graph 3.5）.
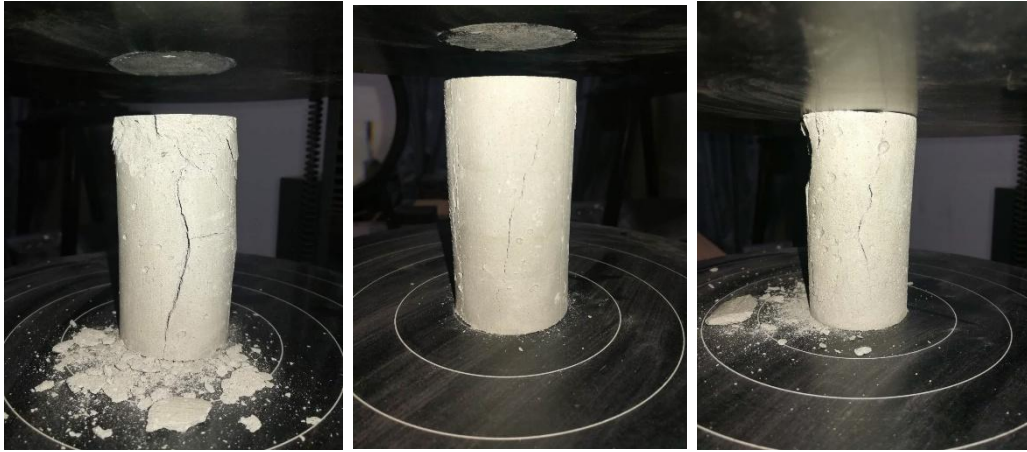
Fig.3.5 Typical failure pictures of some samples

3.3.1 Analyze the orthogonal test result with range method

Based on the parameter of cohesive force, uniaxial compressive strength, elasticity modulus and longitudinal wave velocity, range method (sensitive analysis) is used to prioritize the influences on the physical characteristics of model material generated by the mass ratio of quartz sand and gelatinizer (A), the mass ratio of cement and gypsum (B), the quantity of iron ore powder (C) and water content (D). According to orthogonal theory, firstly, figure out the range first by the average of every factor under different levels. The range is just the average of the biggest and the smallest figure. Secondly, order the ranges obtained from the step mentioned above. If the range is bigger, then the objective parameter will fluctuate greatly with only a small change on relevant values, then the factor can be defined as a sensitive one; If the range is smaller, then the objective parameter will fluctuate slightly with only a small change on relevant values, then the factor can be defined as a non-sensitive one. According to the result of orthogonal test, the influence on the test results could be got through sensitivity analysis by applying range method:

(1) analysis of factors on cohesive force
Figure out the average and the range based on the factors, presented in the orthogonal form, which generated influence on cohesive force of specimen (as shown in the following Tab 3.5). K1, K2, K3, K4 respectively show the experiment result of every factor under four levels; k1, k2, k3, k4 are the average of K1, K2, K3, K4 respectively.

Tab.3.5 Range method analysis of cohesion

NO.	A	B	C	D	Cohesive force/kPa
1	1	1	1	4	108.2
2	1	2	2	3	105.1
3	1	3	3	2	93.4
4	1	4	4	1	91.8
5	2	1	2	2	80
6	2	2	1	1	82.8
7	2	3	4	3	69.8
8	2	4	3	4	73.3
9	3	1	3	1	51.5
10	3	2	4	2	50.1
11	3	3	1	3	62.4
12	3	4	2	4	59.8
13	4	1	4	3	39.1
14	4	2	3	4	30.1
15	4	3	2	1	45.5
16	4	4	1	2	49.5
K_1	388.5	278.8	302.9	271.6	
K_2	277.4	268.1	290.4	273	
K_3	223.8	271.1	248.3	276.4	
K_4	164.2	274.4	250.8	271.4	
k_1	97.125	69.7	75.725	67.9	
k_2	69.35	67.025	72.6	68.25	
k_3	55.95	67.775	62.075	69.1	
k_4	41.05	68.6	62.7	67.85	
Range	56.075	2.675	13.65	1.25	

Comparing the extreme values in the table, the sensitivity of the four factors is ranked as A>C>B>D. The result indicates that the range of mass ratio of quartz sand and gelatinizer (A) is far higher than other factors and is mass ratio of quartz sand and gelatinizer (A) is a sensitive factor; while the range of water content is the smallest one and thus is non-sensitive. In order to reflect the influence of all factors on cohesive force, the different levels of each factor are taken as the X-axis, and the cohesive force as Y-axis to draw the intuitive range analysis graph as shown in Tab 3.6: the cohesive force is affected most by the mass ratio of quartz sand and gelatinizer (A). When the total mass of the specimen is fixed, with the increase of quartz sand content, the content of the cement and gypsum decrease, making it is difficult to completely fix the loose-grained granule and the sand grain shift easily, which greatly reduces the cohesive force with
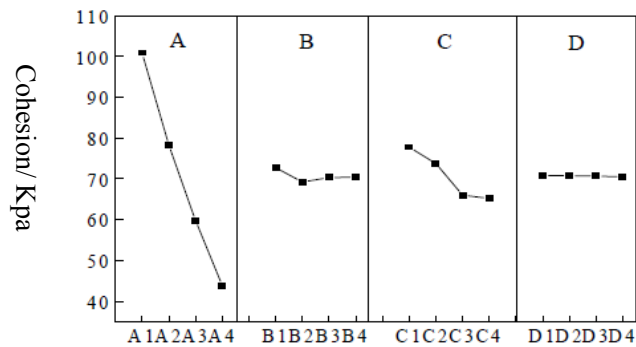

Fig.3.6 Analysis of the factors affecting cohesion

increase of quartz sand content. Similar to the quartz sand, the cohesive force of the specimen slightly decreases with the increase of the amount of iron ore powder. Compared to the 40-item quartz sand, the 400-mesh iron ore powder has a smaller particle size and the effect on the cohesive force thereof is much smaller than that of the quartz sand. Since the specimen is completely dry during test and the strength there of is established after conservation, the water content has little effect on cohesion and is a non sensitive factor.

(2) Figure out the average and the range of compressive strength based on the factors, presented in the orthogonal form, under different levels. As shown in Tab 3.6.

Tab.3.6 Range method analysis of uniaxia compressive strength

Grade	A	B	C	D
1	3.23	2.24	2.53	2.49
2	2.37	2.39	2.56	2.59
3	2.14	2.62	2.63	2.70
4	1.41	2.83	2.69	2.51
Range	1.82	0.59	0.16	0.21

Through analyzing the extreme values in the table above, the sensitivity of the four factors is ranked as A>B>D>C. The result indicates that the mass ratio of quartz sand and gelatinizer (A) is a sensitive factor influencing the uniaxial compressive strength of the specimen, which is followed by the mass of ratio of cement and gypsum (B). The iron ore powder (C) and the water content (D) are two factors causing few effects. The intuitive range analysis graph as shown in Tab 3.7 also shows a similar relations: The compressive strength of the specimen decreases rapidly with the increase of the mass ratio of quartz sand and gelatinizer (A). The quartz sand is a loose-grained granule, and a large number of granules are difficult to establish the strength in the absence of cement and gypsum (B). The stability of internal cementation and the integrity of specimen is low. The compressive strength slightly increases with decreasing proportion of the cement and gypsum (B), that is, compared with gypsum, the effect of cement on the specimen strength is more obvious. Under the same conditions, the increase of cement percentage is helpful to strengthen cementation. The influence of water content (D) on the strength increases first and then decreases. The water is a reactant in the gypsum maturation reaction and the cement hydration reaction. The lack of water causes incomplete chemical reaction, which is not conducive to the cementation between gypsum and cement, affecting the establishment of strength; while too much water will lead to slurry saturation, and the excessive water can not be directly involved into the chemical reaction and exists as free water. The existence of free water is not conducive to the increase of the strength of the specimen during conservation, and the gas generated by the chemical reaction will be attached on the surface of the free water and it is difficult to escape. As a result, there are a large number of pores on the internal and the surface of the dried specimen, which affects the overall strength.
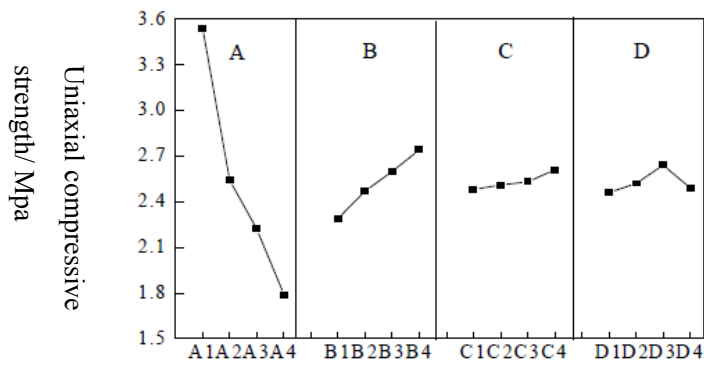
Fig.3.7 Analysis of the factors affecting compressive strength

Figure out the average and the range of elasticity modulus based on the the factors, presented in the orthogonal form, under different levels as shown in Tab 3.7.

Tab.3.7 Range method analysis of elastic modulus

Grade	A	B	C	D
1	1298	902.7	779.1	851
2	974.7	887.4	814.4	867.4
3	730.8	826.5	867.5	877.5
4	324.9	801.5	986.3	886.5
Range	973.1	101.2	207.2	35.5

Through analyzing the extreme values in the table above, the sensitivity of the four factors is ranked as A>C>B>D. The result indicates that the mass ratio of quartz sand and gelatinizer (A) is a sensitive factor, followed by the iron ore powder, influencing the elasticity modulus of the specimen most under different levels. The intuitive range analysis graph as shown in Tab 3.8 also shows that the elasticity modulus is affected most by the mass ratio of quartz sand and gelatinizer (A). The less the proportion of the cement and gypsum is, the little extra force are needed to deform the specimen. When the mass ratio of quartz sand and gelatinizer (A) is more than 2, the shear slip failure will easily occur on specimen.The incorporation of iron ore powder increases the integrity of the specimen because the particle size of the iron ore powder is so small that it is able to effectively fill the pores between among quartz sand particles, which helps cementation and the elasticity modulus of the specimen increases slightly accordingly; the proportion of the cement and gypsum also slightly affects the elastic modulus. Compared with cement, gypsum is more effective for improving the elastic modulus. Under the same conditions, when the gypsum content is high, the elastic modulus of the specimen is larger.
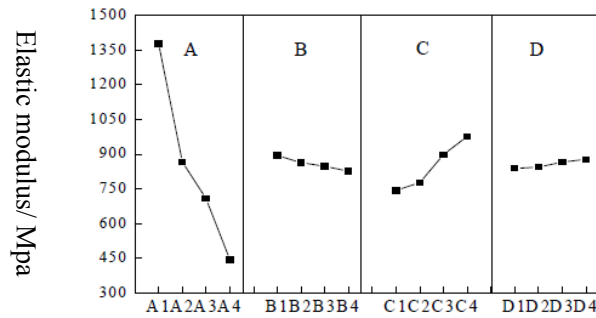
Fig.3.8 Analysis of the factors affecting elastic modulus

(3) analysis of factors on longitudinal wave velocity

Figure out the average and the range of longitudinal wave velocity based on the factors, presented in the orthogonal form, under different levels as shown in Tab 3.8.

Tab.3.8 Range method analysis of longitudinal wave velocity

Grade	A	B	C	D
1	4435.75	3856	3811.75	3929.25
2	3899.25	3956.75	3966.25	3932.75
3	3578	3841	4126	3958.25
4	3214.5	3955	4265.25	3945
Range	1221.25	115.75	453.5	29

Through analyzing the extreme values in the table above, the sensitivity of the four factors is ranked as A>C>B>D. The result indicates that longitudinal wave velocity is affected most by the mass ratio of quartz sand and gelatinizer (A), and then is the proportion of the iron ore powder. The proportion of the cement and gypsum and the water content generates few effects. The intuitive range analysis graph as shown in Tab 3.8 how that the longitudinal wave velocity decreases with the increase of the mass ratio of quartz sand and gelatinizer (A). The high quartz sand content and the lack of gelatinizer contribute to the intra-particle pores are large and the integrity is poor. The transmit of ultrasonic wave is less efficient because of high-frequent reflection and scattering. The transmit process consumes large energy and is low in speed. With the increase of the amount of iron ore powder, the longitudinal wave speed of the specimen has been improved. Because of the large mesh size and the small particle size of iron ore powder, it can effectively fill the pores among the quartz sand particles, thus the compactness of the specimen is

enhanced, which helps the ultrasonic transmission, and increases the longitudinal wave velocity speed; The proportion of the cement and gypsum and the water content generates few effects on the longitudinal wave speed.
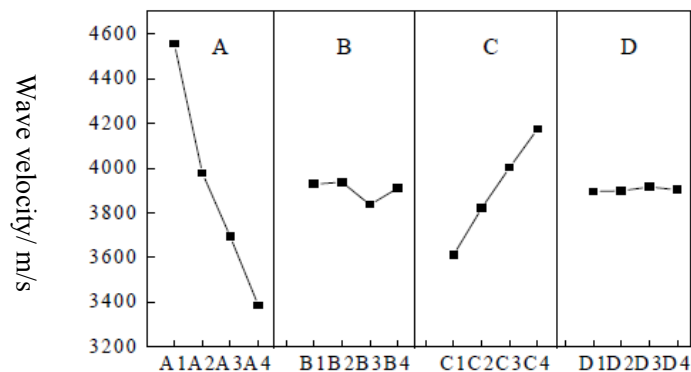

Fig.3.9 Analysis of the factors affecting longitudinal wave velocity

3.3.2 Analyzing test result with variance method

The range analysis method analyzes the results of orthogonal experiments and calculates the average value of the target parameters under different levels of each factor. Through the ranking of the mean value range, the sensitivity analysis of the change of the target parameter to each factor is made. The calculation process is relatively simple and lacks the significance of the influence of factors on the target parameters. Orthogonal test involves four influencing factors, if and only if the value of a certain factor changes, that is, single factor changes, by calculating the test result change, it can be easier to determine the target parameter affected degree; When there are multiple factors that change the value, that is, multi-factor changes, it is difficult to distinguish the influence degree and proportion of each factor on the test result, and then it is impossible to analyze the significance of each factor on the test result. Therefore, in order to compensate for the inadequacy of the analysis method of variance, the variance calculation can not only analyze the independent influence of multiple factors on the target parameters, but also can be used to analyze the significant influence of interactions of different factors on the target parameters, and ultimately be beneficial to the target. The optimal combination of parameters.

According to the results of the orthogonal test, the variance analysis of the basic physical and mechanical parameters of the test piece was carried out and the analysis was performed using the analysis of variance table, as shown in Table 3.9:

Tab. 3.9 Table of variance analysis

Target parameter	Source of variation	Sum of squares of deviations	DOF	RMS	F value	Threshold	Influence
Cohesive force	A	S_A	$f_A = r - 1$	$\bar{S}A = \frac{SA}{fA}$	$FA = \bar{S}A / \bar{S}e$	$F_{1-\alpha}(f_A,\ f_e)$	
Compressive strength	B	S_B	$f_B = r - 1$	$\bar{S}B = \frac{SB}{fB}$	$FB = \bar{S}B / \bar{S}e$	$F_{1-\alpha}(f_B,\ f_e)$	
Elasticity modulus	…	…	…				
Longitudinal wave velocity	…	…	…				
	Error	S_e	f_e		$FA = \bar{S}A / \bar{S}e$		
	Total	S_T	$f_T = n-1$				

The mathematical meaning of the signs referred in the tables and the computing formula are as follow:

S_A, S_B, $\cdots$, is the total sum of square of A and B respectively, $S_j = \sum_{k=1}^{4} 4(\bar{X}_{kj} - \bar{X})^2$, $\bar{X} = \frac{1}{n}\sum_{k=1}^{16} X_k$;

S_T is the total sum of square $S_T = \sum_{k=1}^{16}(X_K - \bar{X})^2$;

S_e is the sum of square of errors, $S_e = S_T - S_A - S_B - \cdots$;

$f_A = f_B = r - 1$ is the DOF of every factors. The DOF is 3 in this orthogonal test.

$f_e = f_T - f_A - f_B - \cdots$ is the error DOF, among which is total DOF. There are 16 groups in this orthogonal test, thus n is 16;

$\overline{S_A} = \frac{S_A}{f_A}$, $\overline{S_B} = \frac{S_B}{f_B}$, …is the RMS, and $\overline{S_e} = S_e/f_e$ is the error sum of square;

Divide mean square $\bar{S}j$ by error mean square $\bar{S}e$, we get F. According to the F distribution function, we carry out a significant analysis of each factor and test the accuracy of orthogonal test. Taking cohesion as an example, the design variance analysis calculation table is shown in table 3.10:

Tab. 3.10 Table of variance calculation

NO.	A	B		D	Cohesive force /kPa
1	1	1	1	4	108.2
2	1	2	2	3	105.1
3	1	3	3	2	93.4
4	1	4	4	1	91.8
5	2	1	2	2	80
6	2	2	1	1	82.8
7	2	3	4	3	69.8
8	2	4	3	4	73.3
9	3	1	3	1	51.5
10	3	2	4	2	50.1
11	3	3	1	3	62.4
12	3	4	2	4	59.8
13	4	1	4	3	39.1
14	4	2	3	4	30.1
15	4	3	2	1	45.5
16	4	4	1	2	49.5

	A	B		D	
$\bar{X}_{1j}$	100.88	72.75	77.78	70.8	
$\bar{X}_{2j}$	78.25	69.25	73.75	70.78	
$\bar{X}_{3j}$	59.78	70.33	66	70.68	$\bar{X} = 70.69$
$\bar{X}_{4j}$	43.85	70.43	62.53	70.5	$S_T = 7760.12$
S_j	7232	26.05	445.75	0.2256	
S_e	$S_e = S_T - S_A - S_B - S_C - S_D = 56.1$				

Taking the calculation results of cohesive force as an example to figure out the sum of squares and errors sum of squared of the uniaxial compressive strength, elasticity modulus, and longitudinal wave velocity at different levels. The results are given in the

form of a variance analysis table as shown in Table 3.11, providing convenience for performing F-test and test accuracy analysis.

Tab. 3.11 Table of variance calculation

Target parameter	Source of variation	Sum of squares	DOF	RMS	F value	Threshold	Significance
Cohesive force /kPa	Factor A	7232	3	2410.67	128.94		***
	Factor B	26.05	3	8.68	0.46	$F_{0.99}(3,3) = 29.5$	
	Factor C	445.75	3	148.58	7.95	$F_{0.95}(3,3) = 9.28$	*
	Factor D	0.2256	3	0.075	0.004	$F_{0.90}(3,3) = 5.39$	
	Error e	56.09	3	18.7			
	Total T	7760.12	15				
Uniaxial compressive strength /MPa	Factor A	6.7	3	2.23	62.6		***
	Factor B	0.44	3	0.147	13.11	$F_{0.99}(3,3) = 29.5$	**
	Factor C	0.057	3	0.019	6.47	$F_{0.95}(3,3) = 9.28$	*
	Factor D	0.0063	3	0.0021	5.53	$F_{0.90}(3,3) = 5.39$	*
	Error e	0.107	3	0.036			
	Total T	7.31	15				
Elasticity modulus /MPa	Factor A	1858329	3	619443	49.45		***
	Factor B	11250	3	3750	0.3	$F_{0.99}(3,3) = 29.5$	
	Factor C	140594	3	46864.7	6.74	$F_{0.95}(3,3) = 9.28$	*

	Factor D	11161	3	3720.3	0.297	$F_{0.90}(3,3)$ $= 5.39$	
	Error e	37579	3	12526.3			
	Total T	2058913	15				
Longitudinal wave velocity/Km/s	Factor A	2.879	3	0.96	25.25		**
	Factor B	0.0255	3	0.0085	0.223	$F_{0.99}(3,3)$ $= 29.5$	
	Factor C	0.697	3	0.232	6.11	$F_{0.95}(3,3)$ $= 9.28$	*
	Factor D	0.00092	3	0.0003	0.0081	$F_{0.90}(3,3)$ $= 5.39$	
	Error e	0.114	3	0.038			
	Total T	3.717	15				

Compared "F" in the chart with standard "F" critical value, belief α adopts 0.01, 0.05 and 0.10. If $F > F_{0.01}(3,3)$, the influence of this factor on the target parameters is highly significant, and it is marked with ***; If $F_{0.05}(3,3) < F < F_{0.01}(3,3)$, the influence of this factor on the target parameters is less significant, it is marked with **; If $F_{0.1}(3,3) < F < F_{0.05}(3,3)$, the significant is less more and more, it marked with *; If $F < F_{0.1}(3,3)$, it doesn't matter so much, we don't mark it.

Comprehensively analyzing the calculation results with range method:

（1）The mass ratio of quartz sand and gelatinizer (A) has a significant effect on the measurement results of the target parameters in orthogonal test. With the increase of the mass ratio of quartz sand and gelatinizer (A), the cohesive force, uniaxial compressive strength, and elasticity modulus of the test specimen tend to decrease significantly. Due to the high content of quartz sand in the specimen, the amount of cement and gypsum is relatively small, and the cementation is not obvious, which results in common 高/低 target parameter values of the specimen. When the mass ratio of quartz sand and gelatinizer (A) is greater than 3, the specimen presents splitting failure and shear slip failure. The overall compactness is low. The mass ratio of quartz sand and gelatinizer (A) also has a significant impact on the longitudinal wave velocity. Large particle size sand hinders the

transmission of ultrasonic wave, and the reflection and scattering among micro particles reduce the transmission efficiency of acoustic wave and further, decreasing the longitudinal wave velocity.

（2）The mass ratio of cement and gypsum (B) mainly affects the uniaxial compressive strength of the specimen. When the content of cement is fixed, properly increasing the proportion of cement components is more effective in strengthening the compressive strength of the specimen. Mixing gypsum with Portland cement helps to delay the coagulating time of cement, which leaves sufficient time to mix components evenly during making the model body. The reaction between gypsum and cement generates ettringite. And is used in the water. The volumetric expansion in the hydration reaction of ettringite compensates the volume shrinkage during the drying process of cement, effectively suppresses cracking on surface the model body, and enhance the integrity.

（3）With increase of the amount of iron ore powder (C), the cohesive force, uniaxial compressive strength, elasticity modulus, and longitudinal wave velocity of the test specimen tend to increase slightly. 400-point iron ore powder can effectively fill the space among 40 mesh quartz sands. With the decrease of porosity in the test specimen, the compactness is improved, and the relevant target parameter values are increased as well. The iron ore powder is designed mainly to increase the saturated unit weight of the model material, so that the similarity ratio of saturated unit weight C_γ is 1. Under the condition of fixed sample volume, it is difficult to incorporate excessive iron ore powder, and the proportion from 15% to 20% is ideal.

（4）The water content (D) has a certain influence on the uniaxial compressive strength of the test specimen and there is also a suitable water volume range. If the water content too little to support the chemical reaction between gypsum and cement to establish cementation strength, and each component is not mixed evenly, it is not conducive to the establishment of strength during the later conservation period; if the water content is large, vadose and stratification mortar will occur during the initial coagulation. Excessive water exists as free water in supersaturated slurries, affecting early strength establishment. When the water content exceeds 35%, the compressive strength of the specimen is significantly reduced, and shows tensile failure because too many internal pores generated by the chemical reactions is attached on the surface of the free water without escaping timely, by which the effect of intensity is greatly affected.

3.4 Determination of dynamic parameters

At the deep national key laboratory of the China University of Mining and Technology (Beijing), the Hopkinson rod impact test was conducted to measure the kinetic parameters of the material. The test environment is shown in Figure 3.10 below. The sample was also prepared according to the ratio of the static orthogonal test scheme, and the sample after 28 days of curing is shown in Figure 3.11 below.
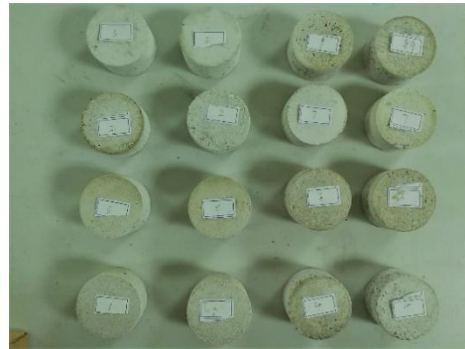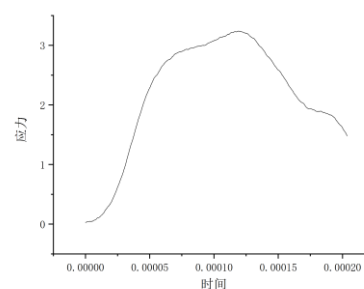

Fig.3.10 State key laboratory   Fig.3.11 Samples of dynamic test

However, because the materials selected for the model test is not strong enough, the reflection wave is difficult to capture, although a complete reflection wave curve can be obtained. There are a lot of clutters, only a very few reflection wave with uniaxial compressive strengths above 3 MPa can be measured completely. After analyzing the data, the resulting stress strain map could be got and shown as in figure 3.12.
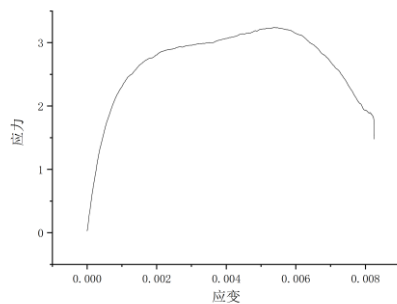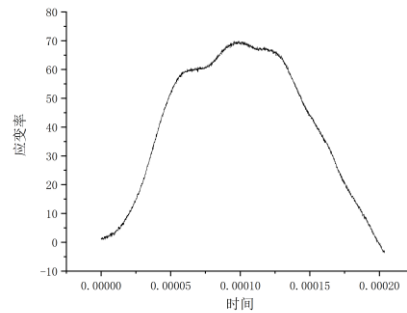

（a）Curve between stress and strain   （b）Curve between stress and time
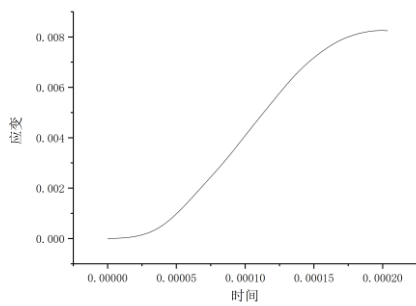
（c）Curve between strain and time　　（d）Curve between strain rate and time

Fig.3.12 dynamic experiment's parameter curve

Because the available specimens which are helpful for searching useful data are not adequate enough, it is difficult to perform effective analysis. However, in the subsequent model tests, the similar materials with higher strength can be produced to determine the dynamics parameters.

3.5 Conclusion

Combining the analytical results of the range analysis method and the variance analysis method, the appropriate range for the distribution ratio of model materials in each group is obtained as follow: the mass ratio of quartz sand and gelatinizer (A) is 1:1 ~ 2:1, the mass ratio of cement and gypsum (B) is 1:1 ~ 2:1, the quantity of iron ore powder (C) is about 15% ~ 20% of the total mass of specimen, and the water content (D) is 30% ~ 35. %. the saturated unit weight of model material is about 23.2 ~ 25.5 kN/m3, cohesive force is 72 ~ 98 kPa, deformation modulus is 750 ~ 1020 MPa, uniaxial compressive strength is 2.72 ~ 3.05 MPa, Poisson's ratio is 0.28 ~ 0.29, longitudinal wave velocity is 4.2 ~ 4.4 km / s. According to similarity ratio, the parameter ranges mentioned above are suitable for the simulation of Class III engineering rock mass, as shown in Table 3.12.

Tab.3.12 Physical mechanical parameters of the grade III engineering rock mass and model material

Component	Unit weight (kN/m3)	Compressive strength(MPa)	Tensile strength (MPa)	Deformation modulus (GPa)	Cohesive force(MPa)	Poisson's ratio	Longitudinal wave velocity(km/s)
grade III engineering rock mass	24.5~26.5	30~60	3.2~4.5	6~20	0.7~1.5	0.25~0.3	3~4.5
Model material	23.2~25.5	2.72~3.05	0.2~0.28	0.75~1.02	0.072~0.098	0.22~0.26	4.2~4.4

Chapter 4: Strength checking and analysis of three dimensional test machine

4.1 Three dimensional modeling for test machine

The common 3D modeling software is Sketch Up, UG, SolidWorks, Pro/E, CATIA and so on. They all have rich 3D solid modeling functions and fine compatibility. They can be used to interface with the common finite element analysis software to realize the exchange and sharing of digital information. The 3D modeling software used in this paper is Sketch Up, which provides many data output formats and can be easily imported into ABQUS for analysis.

4.1.1 Introduction for Sketch Up

Sketch Up is a design tool directly oriented to the creation process of design project. Its creation not only fully expresses the idea of the designer, but also fully satisfies the needs of construction machinery. It enables designers to make a very direct visual creation on the computer, which is an excellent tool for three-dimensional and taking design scheme.

Sketch Up provides a complete CAD, CAE and CAM solution for 3D design, analysis, drawing and processing of products. It belongs to solid modeling software, whose working environment can be two-dimensional or three-dimensional. In a three-dimensional environment, the designer can display his ideas in a realistic model through various methods. Sketch Up constructs basic elements and solid models through the way of point and line. Compared with other specialized and complex modeling software, its obvious feature is that it can automatically identify lines and capture their endpoints to turn line into surface. In addition, it has a large number of plug-ins used to support modeling, which can make up for the lack of hand-painted capabilities of other software systems and greatly reduce the time needed for 3D modeling.

4.1.2 Building model

The bottom-up modeling method is usually used to build 3D models test machines. Firstly, according to the two-dimensional CAD drawings provided by the manufacturer,

the three-dimensional model of the counterforce frame, the main frame, the rear loading frame, the drawbar component, the mechanical mobile device, the rail and the actuators are established by using a single entity in the component modules. In order to simplify the model and speed up numerical calculation, the bolt connection is equivalent to the welded connection. Then, in the assembly module, they are assembled one by one according to the assembly and constraints of each other, and then assembled into a three-dimensional model of the whole geomechanics model.

All parts of the test machine are welded by steel plate and connected by bolt. Although the whole model system looks very complex, it is relatively simple to build, because many of them are characterized by stretching, rotation, mirroring and so on. Complex and advanced features are rare. The detailed modeling process and the overall effect are shown in Figure 4.1.
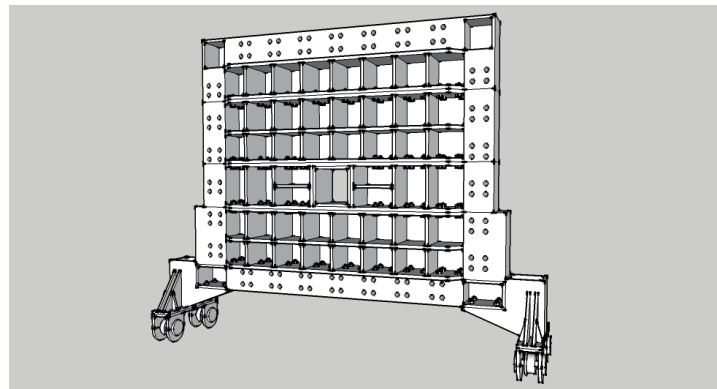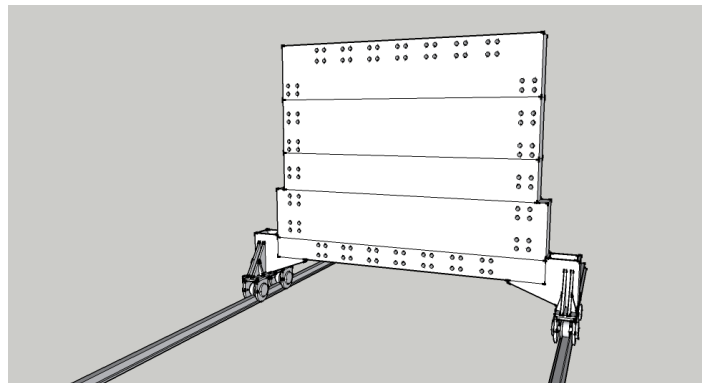

(a) Front counterforce wall of test machine
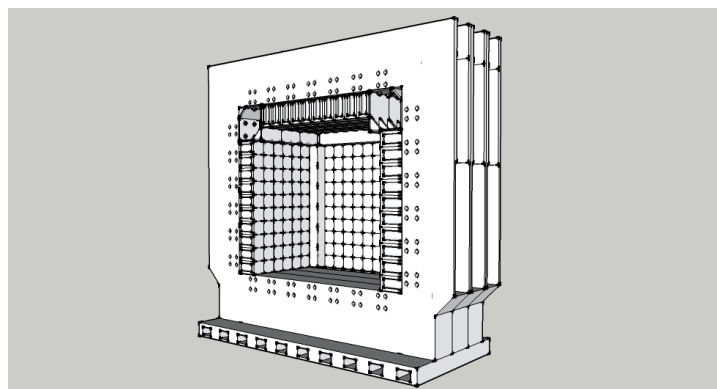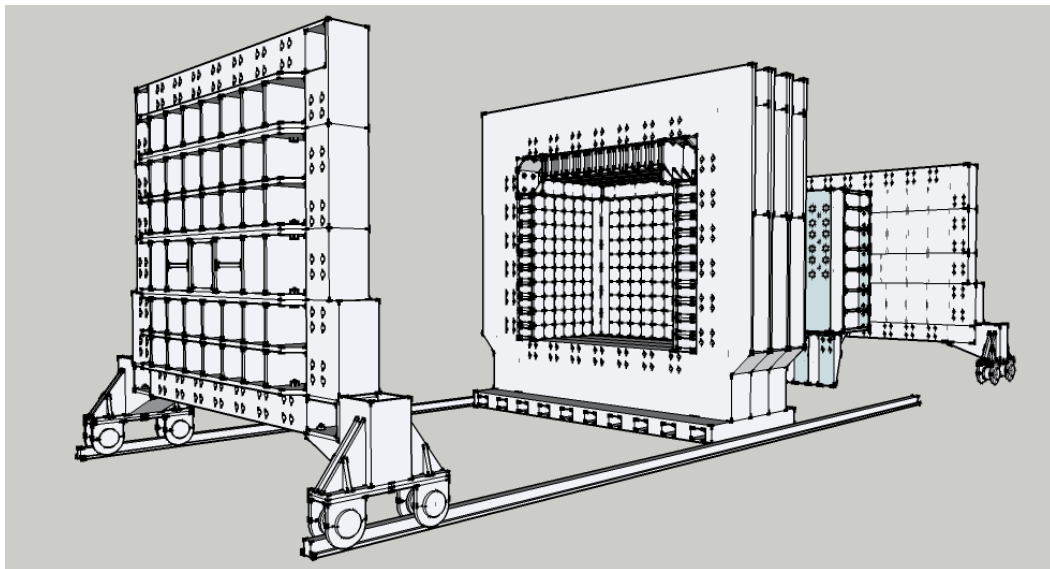

(b) Split-body loading frame of test machine
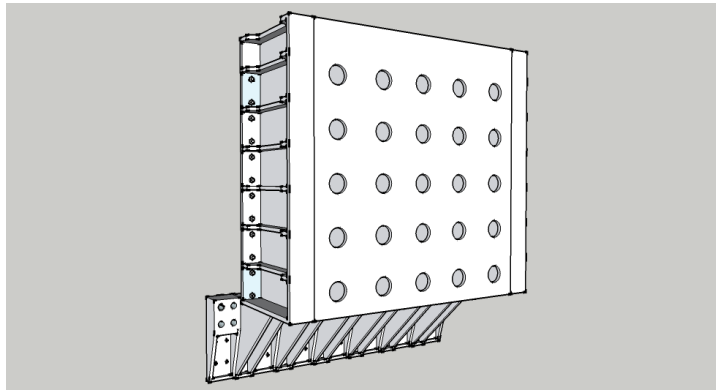
(c) Transition frame of test machine

(d) Back counterforce frame of test machine

(e) Overall structure of the test machine

Fig.4.1 Segment modeling process of test machine

4.1.3 Simplification principles in modeling

Several models are used in the finite element analysis and simulation, so it is necessary to simplify the three-dimensional model of the test machine reasonably according to the characteristics of the virtual prototyping technology and to improve the efficiency of the extreme and analytical processing,

Considering the accuracy of computer simulation analysis and simulation test, the simplification of the test machine structure needs to comply with certain principles.

1. The size of the main parts and components of the testing machine does not change.
2. Secondary parts and partial structures can be simplified.
3. The parts of the main components with little stress can be ignored.
4. The simplified 3D test machine model should be used for finite element analysis and cannot consume too much time.

4.2 Finite element strength analysis of test machine

4.2.1 Introduction of ABQUS

ABAQUS provides users with a wide range of functions and is very easy to use. A large number of complex problems can be easily simulated through different combinations of option blocks. For example, the simulation of complex multi-component problems is achieved by combining the options block defining the geometric size of each component with the corresponding material properties option block. In most simulations and even highly nonlinear problems, the user only needs to provide some engineering data, such as the structural geometry, material nature, boundary conditions and load conditions. In a nonlinear analysis, ABAQUS can automatically select corresponding load increments and convergence limits. It can not only select the appropriate parameters, but also continuously adjust the parameters to ensure accurate solutions in the analysis process. The user can control the numerical results well by defining the parameters accurately. ABAQUS has two main solver modules -- ABAQUS/Standard and ABAQUS/Explicit. ABAQUS also includes a graphical user interface that fully supports the solver, that is, the front and back processing module of human-computer interaction - ABAQUS/CAE. ABAQUS also provides special modules to solve some unique problems. ABAQUS is widely

considered to be the most powerful finite element software, which can be used to analyze complex solid and structural mechanics systems, especially to control large and complex problems and to simulate highly nonlinear problems. ABAQUS can not only do single-part mechanics and multi-physical analysis, but also do analysis and research at system level. The characteristics of ABAQUS's system level analysis are unique to other analytical software. Due to its excellent analytical ability and the reliability of analog complex systems, ABAQUS has been widely used in various industries and research in different countries. Products of ABAQUS play an important role in the research of many high-tech products.

4.2.2 Problems during modeling

In this paper, there are many problems in the finite element analysis of the testing machine as a whole, including the following aspects.

(1) Dimension in finite element analysis

ABAQUS and most other finite element analysis software (such as ANSYS, MSC.MARC, etc.) do not specify the unit of physical quantity. For users, different units can be used for different problems, but it is necessary to ensure the unity of the unit of physical quantity used in the analysis of the same model. However, in practical engineering, many kinds of physical quantity units are often used to describe the problem. In this case, if the finite element analysis is carried out, the expected results are often not obtained. Therefore, we must first carry out the unity of units. This paper adopts the unit of basic physical quantities of mm-t-s-K system.

(2) Import of geometric model

There are two ways to import a good model into ABQUS in Sketch Up: One is to import in the way of parts, which needs to be remodeled again in the whole model of the ABQUS . Although ABQUS has a strong parts assembly capacity, the operation is complicated and time consuming; the other way is to import the model as a whole. Although the overall model will have a deviation of accuracy after importing, as long as it is checked, it is ok to convert it to a precise and effective model.

(3) Simplification of bolt connection

The treatment of bolted connections is one of the many difficulties in finite element analysis. There are three common methods: bonding, contact, and connection. By comparing with the actual situation, the bolts will not be greatly deformed. There is no visible dislocation between the beams and beams, and the bolt connection is simplified as a binding connection to restrict the degree of freedom of the various parts of the

model.

4.3 Analysis of numerical

A complete finite element analysis process consists of three basic steps: pre-processing, analysis and calculation, post-processing. The analysis process of ABQUS is shown in Figure 4.2 below:

```
┌─────────────────────────┐
│ Description of the problem│
└─────────────────────────┘
            │
            ▼
┌─────────────────────────┐
│ Determine the type of analysis│
└─────────────────────────┘
            │
            ▼
┌─────────────────────────┐        ┌──────────┐
│     Solid modeling      │◄───────│          │
└─────────────────────────┘        │          │
            │                       │          │
            ▼                       │          │
┌─────────────────────────┐        │          │
│     Define materials    │        │          │
└─────────────────────────┘        │ Modify   │
            │                       │          │
            ▼                       │          │
┌─────────────────────────┐        │          │
│ Define assemblies, steps,│       │          │
│   outputs, loading      │        └──────────┘
└─────────────────────────┘             ▲
            │                           │
            ▼                           │
┌─────────────────────────┐            │
│   Mesh and Calculation  │            │
└─────────────────────────┘            │
            │                           │
            ▼                           │
┌─────────────────────────┐            │
│   Post processing data  │            │
└─────────────────────────┘            │
            │                           │
            ▼                           │
        ◇ quantified ◇─────────────────┘
            │
            ▼
┌─────────────────────────┐
│    Design and output    │
└─────────────────────────┘
```
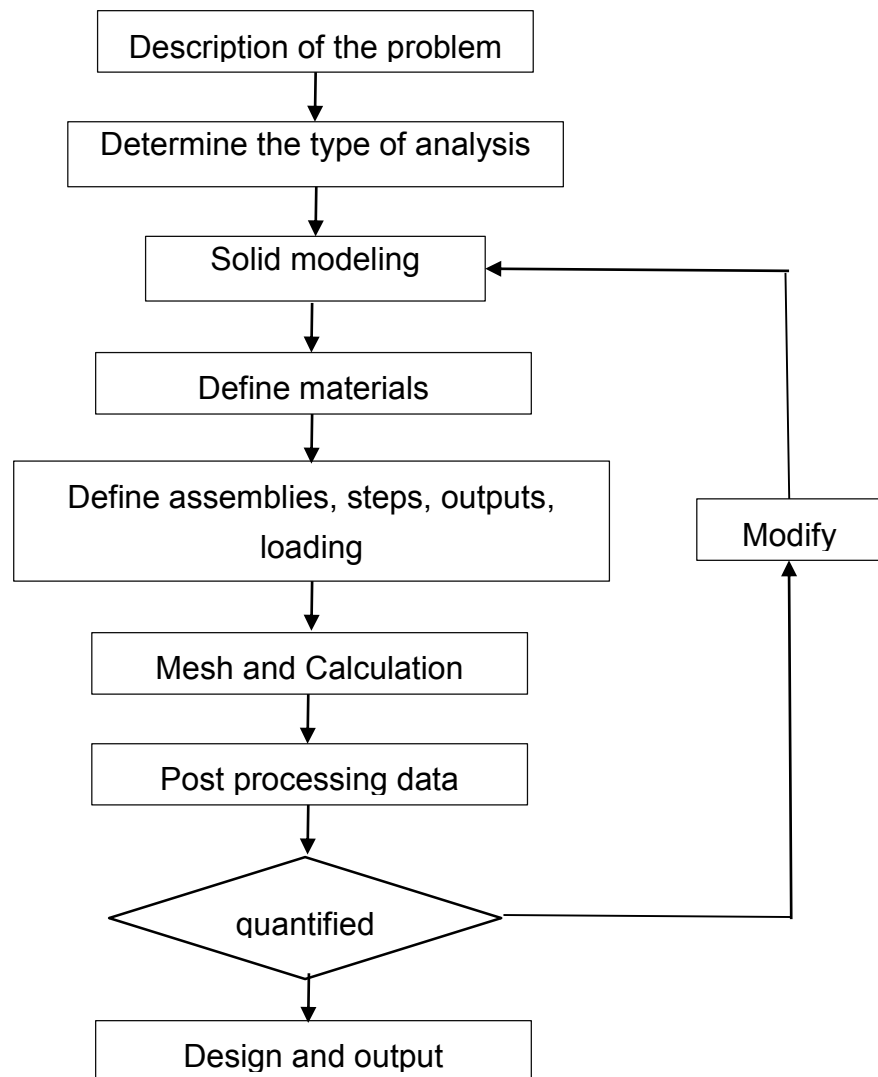
Fig.4.2 ABQUS analysis flow diagram

(1) Define the material properties of the testing machine

According to the design drawings provided by the manufacturer, the steel used in the test machine is Q420. It is a kind of low-alloy high-tensile structural steel. Q420 has high tensile, good fatigue resistance capacity, high tenacity , low brittle transition temperature, good cold forming and welding performance, good corrosion resistance and certain wear resistance. It has high tensile and higher comprehensive mechanical properties especially in normalizing or normalizing plus tempering. In this paper, the main mechanical parameters of Q420 are: Elastic modulus ---200Mpa, Poisson's ratio ---0.28, Density --7.85 g/cm3.

(2) Define analysis steps

The analysis step module is mainly used to define the analyze steps and output. This paper not only involves analysis of structural statics contact, but also involves the analysis of bursting force. Two analysis steps need to be set up. On the other hand, the force of model loading is relatively large, so the separate process of loading can help the convergence of model calculation. The two analytical steps established in this paper are Static General and Dynamic Implicit.

(3) Define interaction

The interaction module is mainly used to define the interactions, constraints and connectors among the parts. In the actual situation, the beams are connected by bolts, but in many tests, there is no case of dislocation and deformation, so it is simplified as a binding connection between the surfaces. Similarly, the connection between stiffened ribs and beams is also simplified as a binding connection. Because the deformation occurred during the test is relatively small to the size of the whole test machine, so this simplification does not have a great effect on the final result.

(4) Define loading and boundary conditions

The purpose of this numerical simulation is to calculate the maximum deformation that the testing machine can bear under the most unfavorable load. In other words,, how much are the dynamic load and static load of the test machine when the test machine is in the limit of deformation. The static load exerting force can provide the test oil source system with maximum pressure 5Mpa. The dynamic load uses different parameters based on different types of explosives. The explosion pressure of RDX is 33.8GPa when the density is 1.767g/cm3, and the detonation pressure is 9.3GPa when apparent density of lead azide is 1.5 g/cm3 (dextrin).

The counterforce wall is connected with the back frame of the main body of test machine through the screw and nut, which runs through the front and back. In the finite element, only the holes around the counterforce wall are required to be constrained. The

six-degree-of-freedom of the surrounding holes are all restrained, so that the boundary conditions can be set.

(5) Mesh

Dividing a reasonable grid is an important step in the finite element analysis, which not only relates to the accuracy and the speed of the solution, but also to the final convergence of the solution. In this paper, the meshing of the counterforce wall of the test machine is shown in Figure 4.3 below.
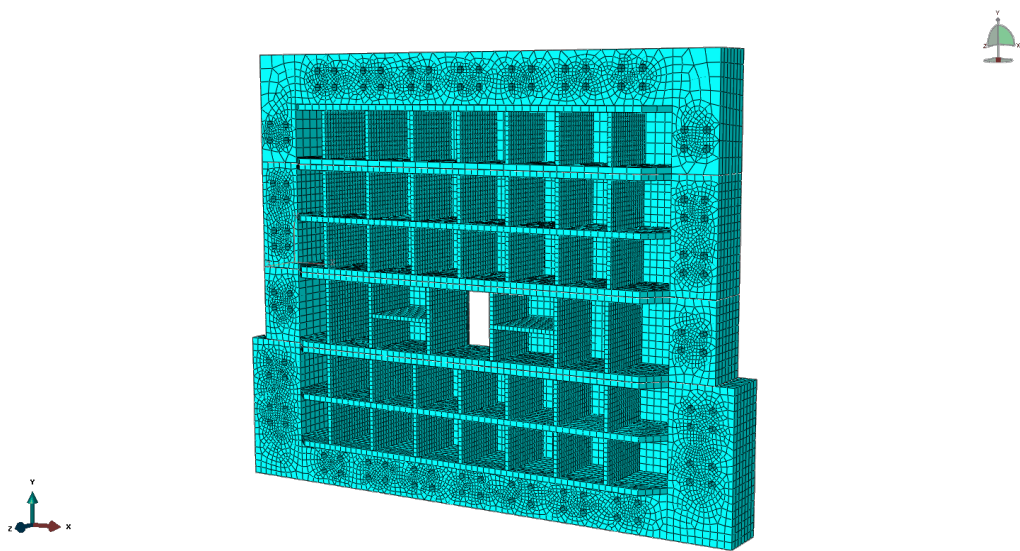

Fig.4.3 mesh generation of reaction wall

Each part of the model uses a unit (C3D8R), which is generally accurate, but is suitable for handling contact problems. The grid is further subdivided near the key beams and around the holes. The size of the partially divided grid away from the key beam is slightly larger, which does not have much effect on the final result, but it can be a significant reduction in the calculation time.

4.3.1 Strength analysis for counterforce wall

The following figure shows the stress cloud diagram on the front and back of the recoil wall of the tester, respectively, as shown in Figures 4.4 and 4.5. It can be seen from the figure that the stress is mainly distributed in the middle and sides of the middle beam and the key beam, and the maximum main stress value is relatively large around the observation window, which is prone to deformation and belongs to an area that emphasizes analysis. The reason is that the waist height of the key beam is relatively

small. Compared with other beams, deformation is more likely. Because the presence of the observation window breaks the integrity of the beam, the perimeter of the observation window will become more fragile. The stress value near the outer ring is larger than that of the inner side of the hole in the round wire bar.

Select four nodes around the observation window to see its maximum principal stress,
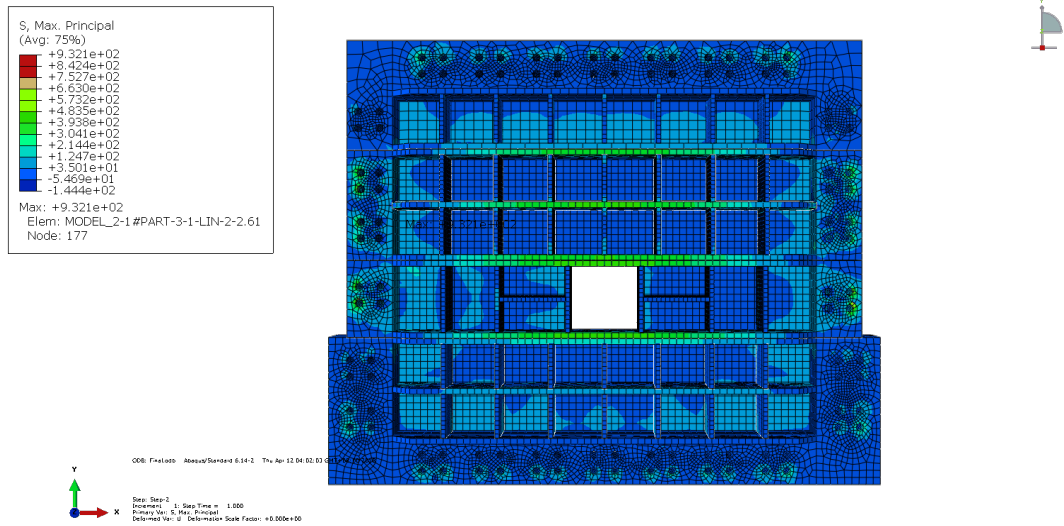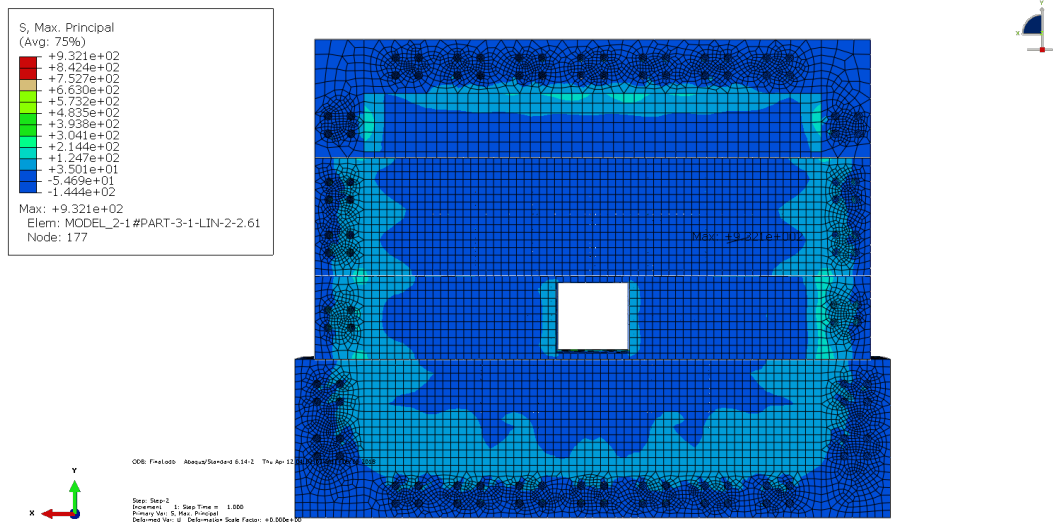

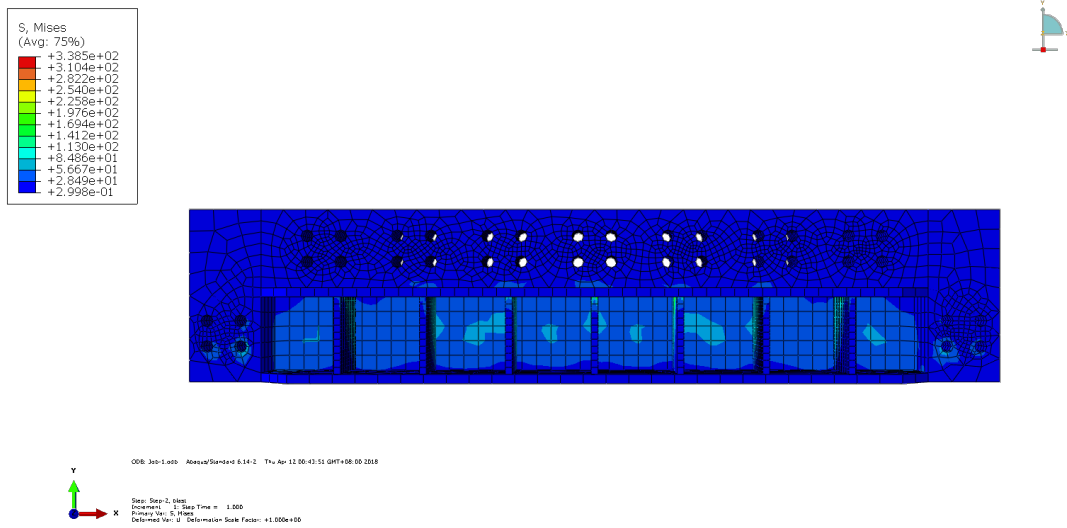Fig.4.4 Front stress contour of reaction wall

Fig.4.5 Back stress contour of reaction wall

Fig.4.6 Mises stress contour of first Beam

4.3.2 First beam deformation analysis

From the Mises stress analysis diagram of the first beam (as shown in Figure 4.6), it can be seen that the stress value in most areas is not very large, and the upper end of the stiffened rib with higher stress has a maximum stress value of 3.38 MPa. Compared with the Q420 steel, the yield stress is much smaller and has little effect on the stability of the entire beam and the reflector frame.
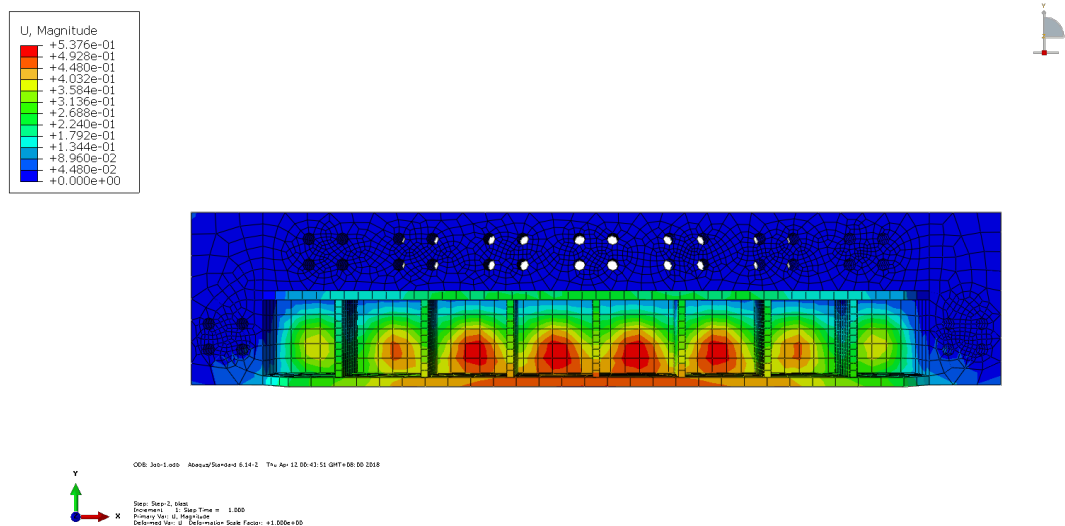

Fig.4.7 Deformation contour of first beam

The cloud diagram shows a displacement vector diagram in the depth direction. From the deformation analysis diagram of the first beam (as shown in Figure 4.7), it can be seen that the deformation is mainly distributed at the lower end of the beam, and

Analysis and Evaluation of Three-dimensional Geology Mechanical Model Experiment   56

the maximum displacement variable is 0.53 mm. Occurs at the lower edge of the beam, node number 436. Compared with the entire model size, the displacement dislocation occurred is small and negligible.

4.3.3 Second beam deformation analysis

From the Mises effort(as shown in Figure 4.8), it can be seen that the stress distribution of the second beam is relatively uniform, and the Mises stress is mainly distributed in the middle part of the front end of the beam, the flange parts on both sides, and the inner hole. The maximum main stress is 1.51 MPa, the node position is 1248, the stress is much smaller than the steel yield stress, the stress level of the entire beam is low, and the structure of the beam is in a stable state.
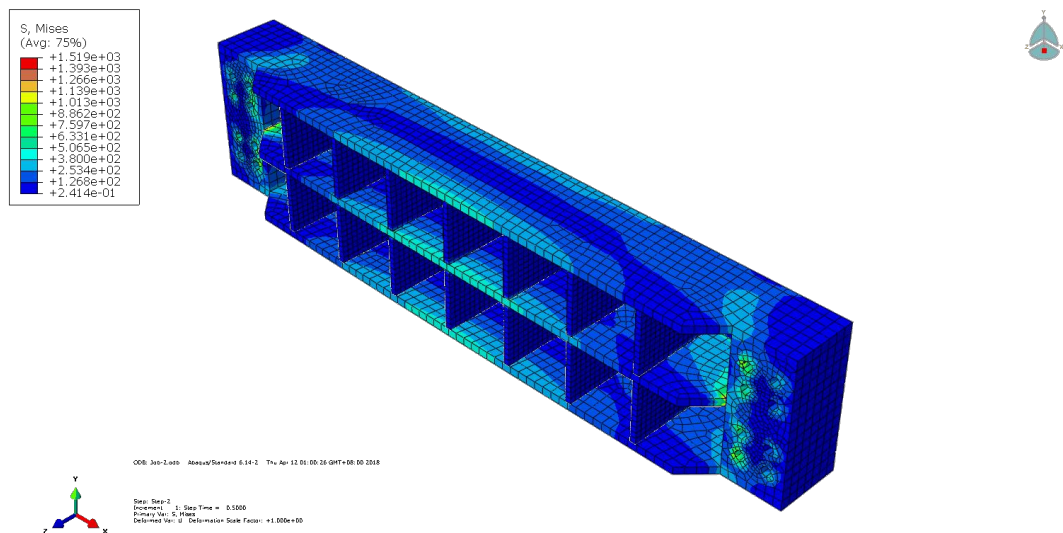

Fig.4.8 Mises stress contour of second Beam

From the deformation analysis of the second beam (as shown in Figure 4.9), it can be seen that the maximum displacement area is still concentrated in the central area, the maximum displacement point is on the panel of the beam, the node number 873, and the maximum displacement is 15.2 mm. Compared with the limit deformation, it is in a safe range. Because the upper and lower interfaces of the beams are bolted to the other two beams, the displacement is limited, and the maximum deformation of the beams is greatly limited.
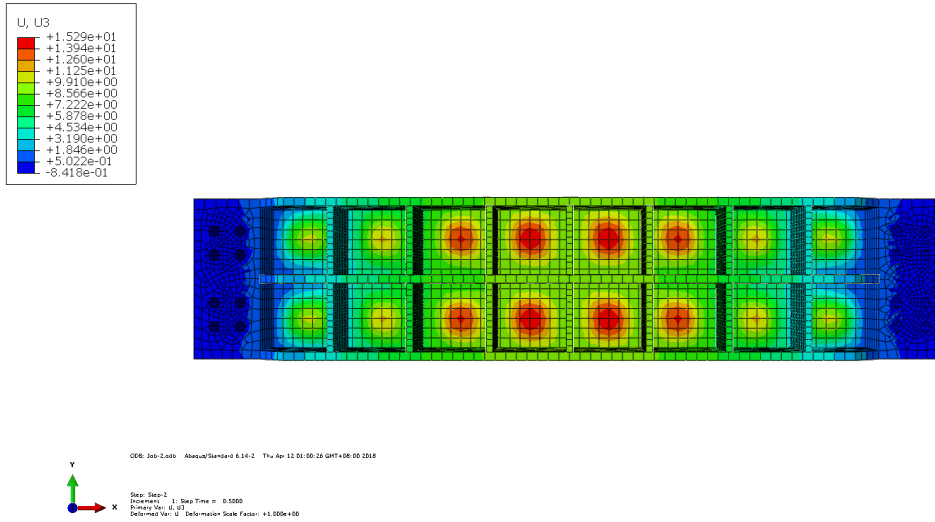
Fig.4.9 Deformation contour of second beam

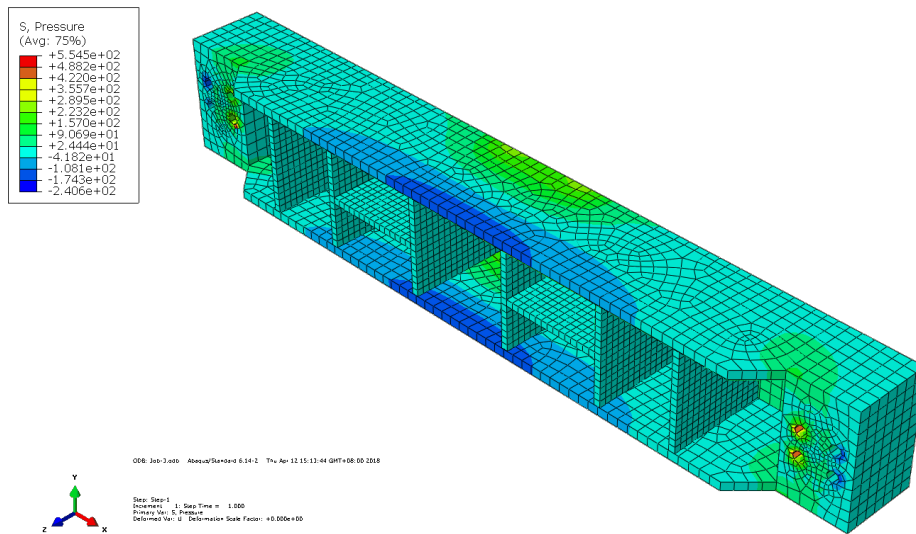## 4.3.4 Key beam deformation analysis

Fig.4.10 Main pressure contour of second Beam

The figure shows a schematic diagram of the force of the key beam 4.10. It can be clearly found that one end near the web is under pressure, one end away from the web is under tension, and the tensile stress is distributed on the upper and lower sides of the observation window. The maximum compressive stress is 5.54 MPa, which occurs at 145 nodes; the maximum tensile stress size is 2.45 MPa, which occurs at 435 nodes. The position of the flange on both sides is the area where the shear stress is concentrated. The maximum shear stress is 1.6 MPa, which is much smaller than the Q420 steel, which is 70 to 90 MPa.
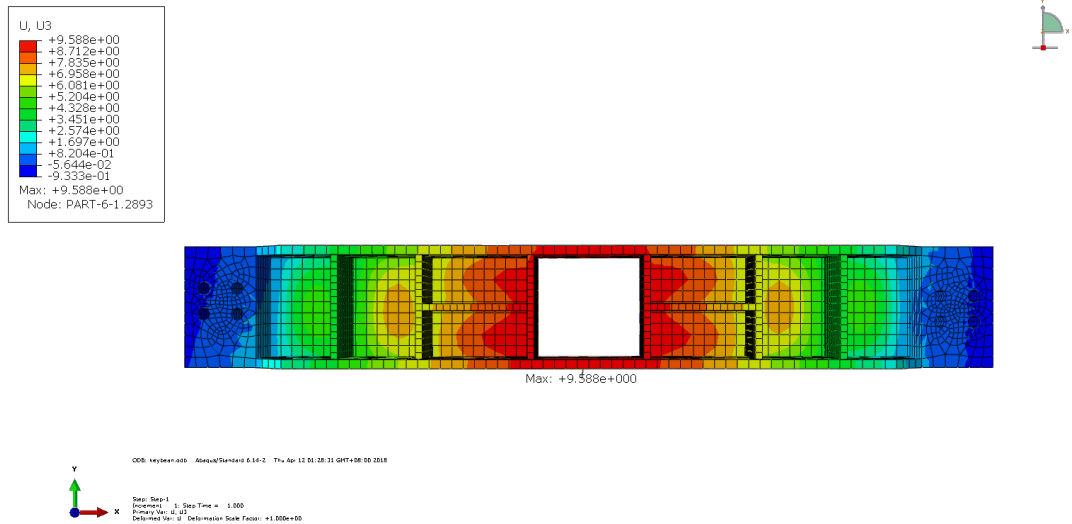
Fig.4.11 Deformation contour of key beam

The figure shows the deformation of the key beam 4.11. The maximum deformation occurs in the middle of the observation window. The node number is 2686 and the maximum form variable is 9.613 mm. Since the presence of the observation window breaks the overall stability of the beam, and the presence of holes causes the model body to form a free surface here, the stress is first released from here, and the shape variable near the hole is the largest, especially the displacement on the node is the largest.

4.3.5 Fouth beam deformation analysis

The force conditions of the fourth beam (as shown in Figure 4.12) are basically the same as the structural design of the first beam, so their stress conditions are basically similar. The maximum principal stress is distributed at the maximum deflection of the beam, and the maximum Mises stress is 2.81 MPa, Occurs at node 155, and the maximum shear stress is distributed near the flange 1.4 MPa, which is much smaller
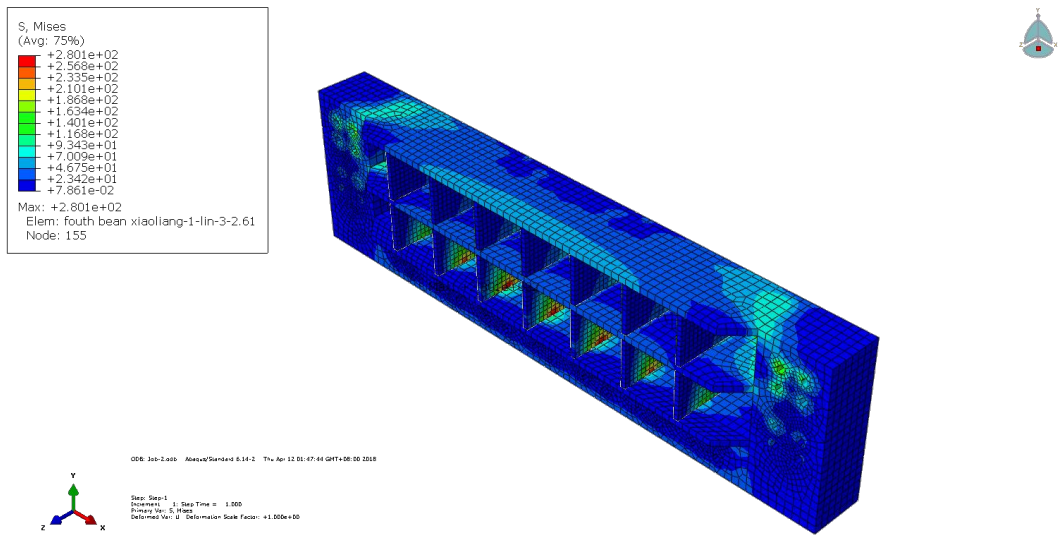
than the yield shear stress of Q420.

Fig.4.12 Mises stress contour of fouth Beam

The deformation form of the fourth beam (as shown in Figure 4.13) is basically the same as the deformation form of the first beam. It occurs within the grid of the beam and the maximum deformation is 2.04 mm. The impact on the steel plate and the overall stability of the steel structure there is no effect.
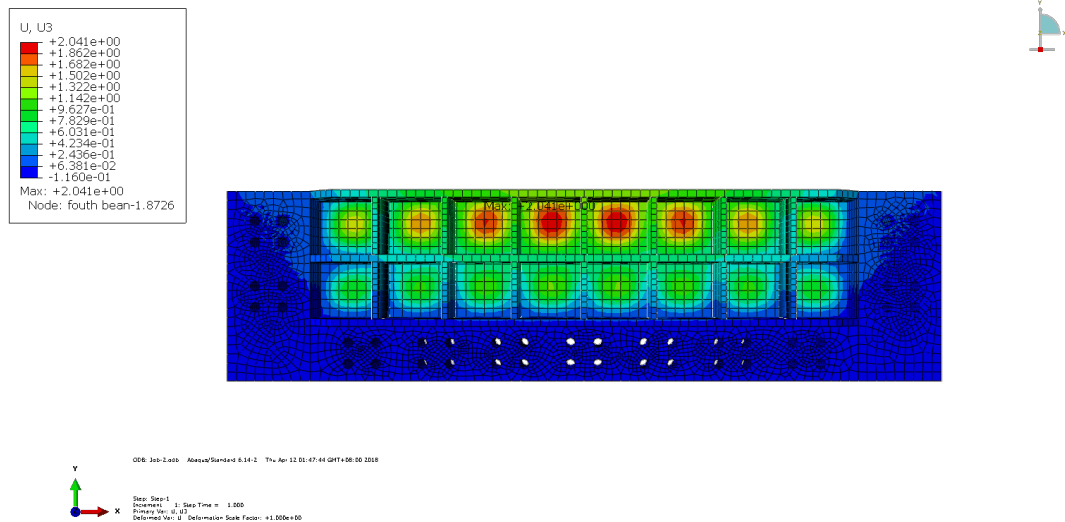

Fig.4.13 Deformation contour of fourth beam

4.4 Conclusion in this chapter

Under the combination of dynamic and static loads, the maximum deformation

generated on the central axis of the tester is similar to the deformation position generated under static conditions, but the numerical value is very different. The maximum deformation is 9mm. However, there is no effect on the overall stability of the testing machine and the normal progress of the test. The simulated environment of the experiment was to try to carry out the blasting of different explosives at a distance of 0.6 m from the observation window. The stress propagation method, through the propagation of the medium, transmitted the blasting stress to the counterforce wall.

Under the action of the static load 5MPa, the maximum main stress is distributed on the vertical central axis, that is, where the maximum deflection of the beam occurs. The maximum deformation is located near the observation window of the key beam, and the deformation is 0.5 mm. It has no effect on the overall stability of the testing machine and the acquisition of test data. The overall stability near the observation window is relatively poor, and there is also a free surface, which is prone to stress concentration areas, so the resulting deformation is also the largest.

Chapter 5: Conclusion and Outlook

5.1 Conclusion

    This paper takes the MCE-3D large-scale mine engineering three-dimensional model system independently researched and developed by China University of Mining and Technology (Beijing) as the main research object. Based on the similarity theory, the model material used in the blasting test is studied, and the physical and mechanical parameters are measured to obtain an appropriate ratio range, and the point of the algorithm analysis of the reaction wall of the test machine, calculate its deformation under the most unfavorable load. The study of the physical and mechanical properties of the model material leads to the following conclusions：

    By analysis of variance method, it was found that the change of the sand-rubber ratio had a significant effect on the measurement results of the orthogonal test target parameters. With the increase of the sand-batch ratio, the cohesion force, uniaxial compressive strength and elastic modulus of the test specimens were all exhibited. There is a clear downward trend. The proportion of cement mainly affects the uniaxial compressive strength of the specimen. When the content of the gel is constant, increasing the ratio of the cement component is more effective for increasing the compressive strength of the specimen. With the increase of the content of iron fine powder, the cohesive force of the specimen, the uniaxial compressive strength, the elastic modulus and the longitudinal wave speed all showed a slight upward trend. The amount of mixing water has a certain influence on the uniaxial compressive strength of the test piece. There is a suitable water volume range, and the mixing water volume is not enough to support the chemical reaction of gypsum and cement to complete the chemical reaction and establish the cementation strength. The mixing of the components is not uniform and is not conducive to the later period. The establishment of strength in the curing process.

    Combining the analytical results of the range difference method and the variance method, an appropriate interval for the distribution ratio of the model materials in each group is obtained. The sand and glue ratio is 1:1 ~ 2:1, the proportion of cement components is 1:1 ~ 2:1, the amount of iron fine powder blended is about 15% ~ 20% of the total mass of the sample, and the mixing water volume is 30% ~ 35. %, with the

above proportions, the model material weight is approximately 23.2 ~ 25.5 kN/m3, cohesive force 72 ~ 98 kPa, deformation modulus 750 ~ 1020 MPa, uniaxial compressive strength 2.72 ~ 3.05 MPa, Poisson's ratio 0.28 ~ 0.29, longitudinal wave speed 4.2 ~ 4.4 km/s. The strength of the test machine calibration study concluded as follows:

（1）Under the static load of 5MPa, the maximum principal stress is distributed on the vertical central axis of the testing machine, that is, where the maximum deflection of the beam occurs, the maximum deformation is located near the observation window of the key beam, and the deformation is 0.5mm, which is stable to the overall test machine. The collection of sexual and experimental data has no effect. The overall stability near the observation window is relatively poor, and there is also a free surface, which is prone to stress concentration areas, so the resulting deformation is also the largest.

（2）Under the combined action of dynamic load and static load, the maximum deformation produced on the center axis of the test machine is similar to the deformation position produced under static conditions, but there is a big difference in value, the maximum deformation is 9mm, but the same There is no effect on the overall stability of the tester and the normal operation of the test. The simulation environment of the test is to try different blasting at a distance of 0.6 m from the observation window. The propagation of stress through the medium propagates the blasting stress to the reaction wall.

5.2 Outlook

This paper systematically introduces the 3D geomechanical model system of China University of Mining and Technology (Beijing). Its innovative and unique features enable more model tests to be performed, especially in dynamic tests. Above, the addition of iron concentrate sand to the test mixture plays a very good role in adjusting the physical and mechanical properties of the material. It provides the basis for future kinetic tests, and can also be achieved as much as possible by adding different components in the model test. The requirements of the material; after checking the strength of the three-dimensional geomechanical model testing machine, the testing machine can withstand a given blasting load. Under the condition of simultaneous dynamic and static loads, it can ensure that the test can be carried out smoothly.

References

[1] HE Manchao, XIE Heping, PENG Suping, JIANG Yaodong. Research on rock mechanics in deep mining[J]. Chinese Journal of Rock Mechanics and Engineering, 2005, 24(16): 2803-2813.

[2] Qian Qihu. The characteristic scientific phenomena of deep rock mass engineering response and the definition of "deep"[J]. East China Institute of Technology, 2004,27(1):1-5.

[3] Nikolaevshij VN.Mechanice of porous and fractured media[M]. NewYork: USA,2010.

[4] Zhou Hongwei, Xie Heping, Zuo Jianping. Research progress of rock mechanical behavior under deep high ground stress[J]. Advances in Mechanics, 2005, 35(1): 91-99.

[5] Qian Qihu. New advances in nonlinear rock mechanics: Some problems in deep rock mass mechanics [A]. In: Chinese Society of Rock Mechanics and Engineering, edited. The 8th National Symposium on Rock Mechanics and Engineering Conference [C]. Beijing: Science Press, 2004: 10-17.

[6] Gu Jincai, Shen Jun, Chen Anmin. Geomechanical model test technology and its engineering application [J]. Proceedings of the China Rock Mechanics and Engineering-Century Achievement Conference, 403-412

[7] Chen Luwang. Physical model test technology research and its application in geotechnical engineering [D]. Wuhan: Institute of Rock and Soil Mechanics, Chinese Academy of Sciences, 2006.

[8] E.FUMAGALLI. Statics and Geomechanics Model [M]. Beijing: Water Power Press, 1979.

[9] R.W.I.Brachman, I.D.Moore, R.K.Rowe. The performance of a laboratory facility for evaluating the structural response of small-diameter buried pipes[J]. Canadian Geotechnical Journal, 2001,38(2):260-275.

[10] Marolo C.Alfaro, Ron C.K.Wong. Laboratory studies on fracturing of low-permeability soils. Canadian Geotechnical Journal,2001,38(2):303-315.

[11] Yan Huiquan, Zhao Deshen. Dynamic simulation of overburden strata mining and research on the technology of filling with stratified belt[J]. Journal of Liaoning Technical University, 2002,21(5): 557-559.

[12] Yan Xinxian. Similar simulation of roof rock movement in caving face[J].

Chinese Journal of Rock Mechanics and Engineering, 2002,21(11):1667-1671.

[13] Wu Yongping, Lai Xingping, Chai Jing. EVOLUTION OF CRACK STABILITY IN LARGE-TILT MECHANICAL MINING AND CAPTURING MINING[J]. Journal of Chang\'an University(Natural Science) 2003,23(3):67-70.

[14] Bai Yiru. Research and application of optical measurement technology for displacement field of similar material model [D]. Doctoral Dissertation of Wuhan Institute of Rock and Soil Mechanics, Chinese Academy of Sciences, 2002.

[15] Deng Kazhong, Ma Weimin, Guo Guangli et al. Physical Simulation of Rock Mass Interface Effect[J]. Journal of China University of Mining & Technology, 1995, 24(4):80-84.

[16] Hu Yaoqing, Zhao Yangsheng, Yang Dong et al. Three-dimensional simulation of roof failure under pressure mining [J]. Chinese Journal of Rock Mechanics and Engineering, 2003,22(8):1239-1243.

[17] R.W.I.Brachman, I.D.Moore, R.K.Rowe. The performance of a laboratory facility for evaluating the structural response of small-diamerer buried pipes[J]. Canadian Geotechnical Journal, 2001,38(2):260-275.

[18] Marolo C.Alfaro, Ron C.K.Wong. Laboratory studies on fracturing of low-permeability soils. Canadian Geotechnical Journal, 2001,38(2):303-315.

[19] Xiao Hongtian, Yang Ruoqiong, Zhou Weibiao. Experimental Study on Subcritical Crack Propagation of Granite in the Three Gorges Shiplock [J]. Chinese Journal of Rock Mechanics and Engineering, 2001, 18(4):12-23.

[20] Zeng Yawu, Zhao Zhenying. Experimental Study on Underground Cavern Model[J]. Chinese Journal of Rock Mechanics and Engineering, 2001,20

[21] Ren Weizhong, Zhu Weishen, Zhang Yujun et al. Experimental Study on the Characteristics of Jointed Surrounding Rock and Its Anchoring Effect under Excavation Conditions [J]. Experimental Mechanics,1997,12(4):514-519.

[22] Liu Jian, Feng Xiating, Zhang Jie et al. Physical simulation of anti-sliding stability in the deep section of the left bank of the Three Gorges Project [J]. Chinese Journal of Rock Mechanics and Engineering, 2002,21(7): 993-998.

[23] Chi Yong, Zhou Jian, Kang Jingyi. Simulation Analysis of Bolt Supporting Coal Roadway Stability[J]. Mining and Metallurgical Engineering, 2002, 22(1)39-41.

[24] Gu Jincai, Shen Jun, Chen Anmin et al. Experimental study on the mechanical model of the stress response of anchorage caverns [J]. Chinese Journal of Rock Mechanics and Engineering, 1999,18(增):1113-1117.

[25] Chen Anmin, Gu Jincai, Shen Jun et al. Model test study on the change law of

the tension tonnage of the anchor cable in soft rock reinforcement over time [J]. Chinese Journal of Rock Mechanics and Engineering, 2002,21(2):251-256.

[26] Zhang Yujun, Sun Yu. Rheological model and calculation method of anchorage rock masses [J]. Chinese Journal of Geotechnical Engineering, 1994,16(3):33-45.

[27] Zhou Xiaomin, Wang Mengshu, Tao Longguang et al. Study on Model Test and Field Measurement of Horizontal Freezing and Excavation of Beijing Metro Tunnel[J]. Chinese Journal of Geotechnical Engineering, 2003, 25(6):666-679.

[28] Zhu Fangcai. Experimental Study on Failure of Similar Material Model under Different Stress Paths[J]. Journal of Central South University of Technology, 2002,33(增):8-13.

[29] Xu Dongjun, Zhang Guang, Li Ting must, et al. Research on Rock Burst Stress State[J]. Chinese Journal of Rock Mechanics and Engineering, 2000, 19(2): 169-172.

[30] Wang Aimin. Development of three-dimensional model and material test instrument [D]. Master thesis of Tsinghua University, 2004.

[31] Ma Fangping, Li Zhongkui, Luo Guangfu. NIOS model material and its application in geomechanical similarity model test [J]. Hydroelectric Power Science, 2004, 23(1): 48-51.

[32] Zhang Qiangyong, Li Shucai, You Chunan. Development and Application of a New Type of Rocky Soil Mechanics Model Test System[J]. China Civil Engineering Journal, 2006, 39(12): 100-107.

[33] Shen Tai, Zou Zhuyin. Research on geomechanical model materials and some experimental techniques [J]. Journal of Yangtze River Scientific Research Institute, 1988, (4): 12-23.

[34] Han Boying, Chen Xialing, Song Yile. Research on Rock-like Materials[J]. Journal of Wuhan Polytechnic University, 1997, 30(2): 6-9.

[35] Zuo Baocheng, Chen Congxin, Liu Caihua. Experimental study on similar materials[J]. Rock and Soil Mechanics, 2004, 25(11): 1805-1808.

[36] Huang Guojun,Zhou Cheng,Zhao Haitao.Integral Stability Three-dimensional Geomechanical Model Test Study on the Niutoushan Double Curvature Arch Dam[J].Northwest Water Power, 2004, 2: 49-52.

[37] Li Tianbin, Xu Jin, Ren Guangming. GEOMETRICAL SIMULATION STUDY ON STRUCTURAL ACTIVITY OF FAULTS IN XI'AN[J]. Journal of Engineering Geology, 1994, 3(2): 34-42.

[38] Lin Yunmei, eds. Experimental rock mechanics [M]. Beijing: Coal Industry Press,

1984.

[39] Gong Zhaoxiong, Chen J. Edited. Rock Mechanics Model Test and Its Application and Development in the Three Gorges Project [M]. Beijing: Water Conservancy and Hydropower Press, 1996.

[40] Zlat.Ko, Langof. Model tests and measurement methods of tunnels in discontinuous media. In: International Symposium on Symposium of Geomechanics, International Society of Rock Mechanics (ISRM). Proceedings of Bergamo, Italy, 1979.

[41] Wang Hanpeng, Li Shucai, Zheng Xuefen. Research progress and engineering application of new geomechanical model test methods [J]. Chinese Journal of Rock Mechanics and Engineering, 2009, 28(1): 2765-2771.

[42] Guo Wenbing, Li Nan, Wang Youkai. Photoelastic simulation study on stress distribution law of surrounding rock of soft rock roadway [J]. Journal of China Coal Society, 2002, 27(6): 596-600.

[43] Wang Xiangqian, Ge Hong. Application of white speckle method in deformation measurement of similar material simulation test [J]. Journal of Chengdu University of Geology, 1989,16(2):109-112.

[44] Ren Weizhong, Zhu Weishen. Application of CCD image processing measurement technology in model test[J]. Hydrogeology and Engineering Geology, 1997,6:56-60.

[45] BAI Yiru, BAI Shiwei, FENG Chuanyu. Improved Automatic Mesh Method to Measure the Model Displacement Field Measurement[J]. Chinese Journal of Rock Mechanics and Engineering, 2003,22(4):543-546.

[46] Ren Weizhong, Yan Xinjian, Ling Haomei. Application of Digital Close-range Photogrammetry in Deformation Measurement of Model Tests[J]. Chinese Journal of Rock Mechanics and Engineering, 2004, 23(3): 436-440.

[47] Hu Shisheng, Wang Daorong, Liu Jianfei. Experimental research on dynamic mechanical properties of concrete materials. Engineering Mechanics, 2001, 18: 115-119.

[48] T E, Ang H Q Shim V P W. An Empirical Strain Rate-Dependent Constitutive Relationship for Glass-Fibre Reinforced Epoxy and Pure Epoxy. Composite Structures, 1995, 33: 201-210.

[49] Yang L M, Shim V P W, Lim C T. A Visco-Hypcrelasitc Approach to Modeling the Constitutive Behavior of Rubber. International Journal of Impact Engineering, 2000, 24: 545-560.

[50] Wang Lili. Stress Wave Foundation. National Defense Industry Press, August 2005 Second Edition: Beijing

[51] Taylor, GI. (1948) "The use of flat ended projectiles for determining yield stress. I: Theoretical considerations" Proc. R. Soc. Lond. A 194 289-299

[52] Davies, R.M. (1948) MA critical study of the Hopkinson pressure bar" Phil. Trans. R. Soc. Lond A 240 375-457

[53] Davies, R.M. (1948) "A simple modification of the Hopkinson pressure bar", in MProc. 7th Int. Cong, on Applied Mechanics: Vol. !H: p. 404.

[54] Boley, B.A. (1955) "Application of Saint Venant's principle in dynamical problems" J. Appl Meek 22 204-206

[55] Hopkinson, J. (1872) "Further experiments on the rupture of iron wire" Proc. Manchest. Liter. Philos. Soc. 12 119-121

中国矿业大学 (北京)

China University of Mining & Technology-Beijing

Thesis Grade

Thesis topic: **Analysis and Evaluation of Three-dimensional Geology Mechanical Model Experiment**

Author: Yuantong Zhang

Supervisor	Renshu Yang	Grade 92	signature
Co-supervisor	Tobias Ladinig	Grade	signature